NORTH ATLANTIC TREATY ORGANIZATION

SCIENCE AND TECHNOLOGY ORGANIZATION

AC/323(SCI-255)TP/759

www.sto.nato.int

STO AGARDograph 300 **AG-300-V30**
Flight Test Technique Series – Volume 30

High Altitude Rotary Wing Flight Testing – Considerations in Planning Rotary Wing Performance Testing for High Altitude Operations

(Essais en vol de voilure tournante à haute altitude – Considérations pour la planification des essais de performance des voilures tournantes pour les opérations à haute altitude)

This AGARDograph has been sponsored by the Systems Concepts and Integration Panel.

Published February 2018

NORTH ATLANTIC TREATY ORGANIZATION

SCIENCE AND TECHNOLOGY ORGANIZATION

AC/323(SCI-255)TP/759

www.sto.nato.int

STO AGARDograph 300 **AG-300-V30**
Flight Test Technique Series – Volume 30

High Altitude Rotary Wing Flight Testing – Considerations in Planning Rotary Wing Performance Testing for High Altitude Operations

(Essais en vol de voilure tournante à haute altitude – Considérations pour la planification des essais de performance des voilures tournantes pour les opérations à haute altitude)

This AGARDograph has been sponsored by the

Systems Concepts and Integration Panel.

The NATO Science and Technology Organization

Science & Technology (S&T) in the NATO context is defined as the selective and rigorous generation and application of state-of-the-art, validated knowledge for defence and security purposes. S&T activities embrace scientific research, technology development, transition, application and field-testing, experimentation and a range of related scientific activities that include systems engineering, operational research and analysis, synthesis, integration and validation of knowledge derived through the scientific method.

In NATO, S&T is addressed using different business models, namely a collaborative business model where NATO provides a forum where NATO Nations and partner Nations elect to use their national resources to define, conduct and promote cooperative research and information exchange, and secondly an in-house delivery business model where S&T activities are conducted in a NATO dedicated executive body, having its own personnel, capabilities and infrastructure.

The mission of the NATO Science & Technology Organization (STO) is to help position the Nations' and NATO's S&T investments as a strategic enabler of the knowledge and technology advantage for the defence and security posture of NATO Nations and partner Nations, by conducting and promoting S&T activities that augment and leverage the capabilities and programmes of the Alliance, of the NATO Nations and the partner Nations, in support of NATO's objectives, and contributing to NATO's ability to enable and influence security and defence related capability development and threat mitigation in NATO Nations and partner Nations, in accordance with NATO policies.

The total spectrum of this collaborative effort is addressed by six Technical Panels who manage a wide range of scientific research activities, a Group specialising in modelling and simulation, plus a Committee dedicated to supporting the information management needs of the organization.

- AVT Applied Vehicle Technology Panel
- HFM Human Factors and Medicine Panel
- IST Information Systems Technology Panel
- NMSG NATO Modelling and Simulation Group
- SAS System Analysis and Studies Panel
- SCI Systems Concepts and Integration Panel
- SET Sensors and Electronics Technology Panel

These Panels and Group are the power-house of the collaborative model and are made up of national representatives as well as recognised world-class scientists, engineers and information specialists. In addition to providing critical technical oversight, they also provide a communication link to military users and other NATO bodies.

The scientific and technological work is carried out by Technical Teams, created under one or more of these eight bodies, for specific research activities which have a defined duration. These research activities can take a variety of forms, including Task Groups, Workshops, Symposia, Specialists' Meetings, Lecture Series and Technical Courses.

The content of this publication has been reproduced directly from material supplied by STO or the authors.

Published February 2018

ISBN 978-92-837-2085-0

AGARDograph Series 160 & 300

Soon after its founding in 1952, the Advisory Group for Aerospace Research and Development (AGARD) recognized the need for a comprehensive publication on Flight Test Techniques and the associated instrumentation. Under the direction of the Flight Test Panel (later the Flight Vehicle Integration Panel, or FVP) a Flight Test Manual was published in the years 1954 to 1956. This original manual was prepared as four volumes: 1. Performance, 2. Stability and Control, 3. Instrumentation Catalog, and 4. Instrumentation Systems.

As a result of the advances in the field of flight test instrumentation, the Flight Test Instrumentation Group was formed in 1968 to update Volumes 3 and 4 of the Flight Test Manual by publication of the Flight Test Instrumentation Series, AGARDograph 160. In its published volumes AGARDograph 160 has covered recent developments in flight test instrumentation.

In 1978, it was decided that further specialist monographs should be published covering aspects of Volumes 1 and 2 of the original Flight Test Manual, including the flight testing of aircraft systems. In March 1981, the Flight Test Techniques Group (FTTG) was established to carry out this task and to continue the task of producing volumes in the Flight Test Instrumentation Series. The monographs of this new series (with the exception of AG237 which was separately numbered) are being published as individually numbered volumes in AGARDograph 300. In 1993, the Flight Test Techniques Group was transformed into the Flight Test Editorial Committee (FTEC), thereby better reflecting its actual status within AGARD. Fortunately, the work on volumes could continue without being affected by this change.

An Annex at the end of each volume in both the AGARDograph 160 and AGARDograph 300 series lists the volumes that have been published in the Flight Test Instrumentation Series (AG 160) and the Flight Test Techniques Series (AG 300) plus the volumes that were in preparation at that time.

High Altitude Rotary Wing Flight Testing – Considerations in Planning Rotary Wing Performance Testing for High Altitude Operations

(STO-AG-300-V30)

Executive Summary

Performance charts for helicopters deployed by the NATO members were generated by flight tests scoped to cover altitudes relevant to the anticipated mission environments. The methods used to generate those graphs were robust and the models well-behaved given the domain of interest. However, during deployment of NATO aircraft to Afghanistan over the last 15 years, extremes of temperature at high altitudes were outside the domains of the models. The combined effects of weight and temperature extremes at high altitude are often not captured by these established methods of test. As a result, the actual performance is often less than that presented in the flight manual. Present approaches must be modified to capture those effects and further define the aircraft's generalized power available and power required model.

The generalized data models for power available and power required are analysed at the extremes of temperature as altitudes approach the limit where supplemental oxygen is used. The compressor reaches a limit bounded by the maximum total pressure ratio, P_{t3}/P_{t2}, attainable across the compressor. Past this limit, the pressure ratio across the compressor will decrease rapidly as will the mass flow rate. This limit is called the surge limit and must be defined during flight test. Temperature at higher altitudes affects the power required model in two ways. The rotor system reaches an aerodynamic limit when a critical amount of the retreating blade stalls or when the Mach effects on the advancing blade cause a large drag rise on the blade and increases the profile drag of the rotor system. Temperature effects at high altitude can create conditions conducive to vortex ring state.

Engine assessment at extreme temperature conditions and high altitudes will define the conditions in the generalized model where the surge boundary occurs. Two methods exist for determining blade stall boundaries. One defines the relationship between the blade loading coefficient and the advance ratio. Varying airspeed, referred weight (W/s) and rotor rpm provides data that defines where the blade stall boundary occurs. Once this boundary is known, it can be used to predict the limiting airspeed at a given weight and rotor rpm. The Equivalent Retreating Tip Speed or ERiTS method uses an approach similar to one used to generalize the stall speed of fixed-wing aircraft. A standard mission gross weight is chosen. Airspeed, referred weight, and rotor rpm are varied and a structural indication of blade stall is used to verify a mathematical model. Given a mission weight, altitude, and rotor rpm, an operator can determine the stall limit of the aircraft and determine the total power required for the limiting case. Many test techniques have been developed to determine the vortex ring state boundary of a helicopter; the paper references those papers.

An understanding of the effects of temperature extremes at high altitude can inform the test organization about the choice of the scope and methods for accurately capturing data to verify power required and power available performance charts for high altitude operations.

Essais en vol de voilure tournante à haute altitude – Considérations pour la planification des essais de performance des voilures tournantes pour les opérations à haute altitude

(STO-AG-300-V30)

Synthèse

Les graphiques de performance des hélicoptères déployés par les membres de l'OTAN ont été produits à l'aide d'essais en vol à des altitudes pertinentes pour les environnements de mission prévus. Les méthodes employées afin d'établir ces graphiques étaient robustes et les modèles bien adaptés au domaine concerné. Toutefois, les aéronefs de l'OTAN déployés en Afghanistan ces 15 dernières années ont rencontré à haute altitude des conditions extrêmes de température sortant du champ des modèles. Il est fréquent que ces méthodes d'essai courantes ne tiennent pas compte des effets combinés du poids et des températures extrêmes lors du vol à haute altitude. Les performances réelles sont donc souvent inférieures à celles indiquées dans le manuel de vol. Les approches actuelles doivent être modifiées pour intégrer ces effets et définir plus précisément la puissance globale disponible et le modèle de puissance nécessaire de l'aéronef.

Les modèles de données génériques relatifs à la puissance disponible et à la puissance nécessaire sont analysés aux extrêmes de température, lorsque l'altitude s'approche de la limite où l'apport d'oxygène est nécessaire. Le compresseur atteint une limite liée au rapport de pression totale maximum, P_{t3}/P_{t2}, qui peut être obtenu dans le compresseur. Passée cette limite, le rapport de pression dans le compresseur diminuera rapidement, tout comme le débit massique. Cette limite est appelée limite de pompage et doit être définie pendant l'essai en vol. La température à haute altitude modifie de deux façons le modèle de la puissance nécessaire. Le système de rotor atteint une limite aérodynamique lorsqu'une portion critique de la pale reculante décroche ou lorsque l'effet Mach sur la pale avançante provoque une forte hausse de la traînée de la pale et augmente la traînée de profil du système de rotor. La température à haute altitude peut créer des conditions propices à la formation d'un anneau tourbillonnaire.

L'évaluation du moteur en conditions de température extrême et à haute altitude définira les conditions du modèle générique dans lesquelles la limite de pompage survient. Il existe deux méthodes pour déterminer la limite de décrochage des pales. La première consiste à définir la relation entre le coefficient de charge de pale et le paramètre d'avancement. La vitesse anémométrique, la masse de référence (W/s) et le régime du rotor qui varient fournissent des données qui définissent la zone dans laquelle la limite de décrochage des pales est atteinte. Une fois que cette limite est connue, elle peut servir à prédire la vitesse anémométrique limite pour une masse et un régime de rotor donnés. L'autre méthode, appelée ERiTS (*Equivalent Retreating Tip Speed*) suit une approche similaire à celle utilisée pour généraliser la vitesse de décrochage des aéronefs à voilure fixe. Un poids total en charge de mission standard est choisi. La vitesse anémométrique, la masse de référence (W/s) et le régime du rotor sont modifiés et une indication structurelle du décrochage de pale sert à vérifier un modèle mathématique. Avec un poids, une altitude et un régime de rotor donnés en mission, un opérateur peut déterminer la limite de décrochage de l'aéronef et la puissance totale nécessaire pour le cas limite. De nombreuses techniques d'essai ont été développées pour déterminer la limite de formation d'un anneau tourbillonnaire d'un hélicoptère ; l'article les cite en référence.

La compréhension des effets des températures extrêmes à haute altitude peut informer l'organisation chargée des essais sur la portée et les méthodes adaptées à un enregistrement précis des données, dans le but de vérifier les graphiques de performance de la puissance requise et de la puissance disponible dans les opérations à haute altitude.

Acknowledgements

The authors are indebted to John Tritschler, David Lee, John Powell, and Derek Gowanlock for their insightful review and comments. A special thanks to Dean Moore who provided the guidance and the contents of the summary.

Foreword

Objective(s):

Established performance test techniques for rotary wing aircraft produce a generalized performance model. The combined effects of weight and temperature extremes at high altitude are often not captured by these established methods of test. As a result, the actual performance is often less than that presented in the flight manual. This AGARDograph explains the effects and their causes and provides approaches to capture those effects and further define the aircraft's generalized power available and power required model.

Topics to be Covered:

Topics to be covered include the generalized performance model for power available and power required, a discussion of the factors that limit power available, the blade stall and compressibility manifestations of weight, temperature and pressure (high altitude), vortex ring state and the approaches to define blade stall and compressibility boundaries.

Preface

John O'Connor, Chief of Academics, U.S. Naval Test Pilot School. Mr. O'Connor is an engineering test pilot with over 3000 hours in 80+ helicopter, tactical jet, and multi-engine aircraft. He holds a B.S. in Mechanical Engineering and an M.S. in Aeronautical Engineering. He is a 1986 graduate of the U.S. Naval Test Pilot School. He has over thirty years of defence acquisition experience and has held executive level positions in research planning; program management; and aircraft manufacturing, production, and repair. He has professional education experience as a college math teacher, graduate-level engineering lecturer, test pilot school academic instructor and test pilot flight instructor.

Jim McCue recently retired as the Senior Rotary-wing Aerodynamics Instructor at U.S. Naval Test Pilot School. Mr. McCue is a Naval Air Systems Command fellow and holds a B.S. and M.S. in Aeronautical Engineering from Virginia Polytechnic and State University. He has served as a Flight Test Engineer and Test Pilot School instructor since 1967. He graduated from U.S. Naval Test Pilot School in 1970. He has contributed, both directly and indirectly, to virtually all major NAVAIR flight test programs over the past 47 years. He made direct contributions to recent flight test development efforts for the F/A-18E/F Super Hornet and the V-22 Osprey. His recommendations regarding aerodynamic modifications and operational techniques to mitigate deficiencies directly enhanced the safety and mission effectiveness of these platforms.

LtCdr John Holder RN, graduated from University College London with a B.Sc (Hons) in Geography. He served in Royal Navy for 21 years as a maritime pilot predominantly flying over 1000 hours in Sea King (H-3) and over 1000 hours in Merlin (AW-101). He attended Empire Test Pilots' School Graduate Rotary Wing Course 46. He has flown over 80 type/model/series aircraft and conducted First of Class dynamic interface flight trials. He was the project pilot and first military pilot to fly new Merlin Mk2. He conducted numerous other trials in Merlin, Sea King, Lynx, Gazelle, Chinook (H-47), and Apache. He is currently on exchange as staff at USNTPS, teaching on Blackhawk, Lakota and Kiowa.

Bryan Carrothers has a Bachelor of Engineering in Engineering and Management from the Royal Military College of Canada and a Master of Science in Flight Test and Evaluation from the National Test Pilot School in Mojave, California. He completed 25 years of service in the Royal Canadian Air Force as a pilot with the last half of his military career as a helicopter test pilot, primarily on the CH146 Griffon and CH147 Chinook helicopters. He is currently working as a Research Test Pilot at the National Research Council Canada.

Table of Contents

		Page
AGARDograph Series 160 & 300		**iii**
Executive Summary		**iv**
Synthèse		**v**
Acknowledgements		**vi**
Foreword		**vii**
Preface		**viii**
Table of Contents		**ix**
List of Figures		**xi**
List of Acronyms and Symbols		**xii**
Author Contact Information		**xiv**
1.0	**Introduction**	**1**
1.1	Mishaps Caused by Weight, Altitude, and Temperature Effects	1
2.0	**Model for Power Available**	**1**
2.1	Standard Limiting Factors	1
2.2	Engine Pressure Ratio (EPR) Limiting	5
2.3	Effects of Compressor Pressure Ratio Limiting	5
3.0	**Model for Power Required**	**7**
3.1	Standard Model Variables	7
3.2	Blade Aerodynamics	8
3.3	Blade Stall	9
3.4	Compressibility at the Blade Tips	9
4.0	**Influences of Weight, Temperature, and Altitude on Power**	**12**
4.1	Hover: Influences of Weight and Temperature, Hot and Cold	12
4.2	Forward Flight: Influences of Weight, Blade Stall, and Compressibility	15
4.3	Climb/Descent: Influences of Blade Stall on Climb/Descent Speeds	17
4.4	Maneuvering Flight: Influences of Blade Stall and Compressibility	18
5.0	**Vortex Ring State**	**21**
5.1	Vortex Ring State Scenario	21
5.2	Vortex Ring State Parameters	21
5.3	Vortex Ring State Testing	22

6.0 Blade Stall Testing 22
6.1 Blade Loading Coefficient 22
6.2 Equivalent Retreating Tip Speed (ERiTS) 23

7.0 Compressibility 23
7.1 A Mention of Referred Weight, Referred True Airspeed and Referred Rotor RPM 23

8.0 Summary 25

9.0 References 27

Annex A – AGARD, RTO and STO Flight Test Instrumentation and Flight Test Techniques Series A-1

List of Figures

Figure		Page
Figure 1	Inlet Recovery Relationships	2
Figure 2	Generalized Engine Parameters	3
Figure 3	Blade Element Diagram of a Compressor Rotor Showing Three Different Flow Conditions	4
Figure 4	Pressure Ratio ~ Wing Lift Analogy	5
Figure 5	User's Chart Showing Loss of Torque at Temperature Extremes	5
Figure 6	Engine Compressor Performance Map	6
Figure 7	Power Required Elements	7
Figure 8	Dissymmetry of Lift in Blade Stall	8
Figure 9	Dissymmetry of Lift from Compressibility Effects	10
Figure 10	Formation of Shock Waves	11
Figure 11(a)	Rotor Map-Simultaneous Stall and Compressibility Conditions in Forward Flight	11
Figure 11(b)	Shock-Induced Drag Rise	12
Figure 12	Aerodynamic Drag as a Function of Mach and Angle of Attack (Subsonic Airfoil)	13
Figure 13	Increase in Hover Power Required and Power Available with an Increase in Weight	13
Figure 14	Effect of Temperature on Hover Power Available and Power Required – No Compressibility Effect	14
Figure 15	Effect of Temperature on Hover Power Available and Power Required – With Compressibility Effect	14
Figure 16	Increase in Power Required with Increased Weight (Forward Flight)	15
Figure 17	Effect of High Temperature (Decreased Density) on Power Required and Available (Forward Flight)	16
Figure 18	Effect of High Temperature (Decreased Density) with Blade Stall on Power Required (Forward Flight)	16
Figure 19	Effect of Low Temperature (Compressibility) on Power Required and Pressure Ratio Limiting on Power Available (Forward Flight)	17
Figure 20	Energy Management Diagram-Zero Angle of Bank	18
Figure 21	Energy Management Diagram-45 Degree Angle of Bank	19
Figure 22	E-M Diagram, Sea Level, Standard Day	20
Figure 23	E-M Diagram, 6K Feet, Standard Day	20
Figure 24	Blade Loading Coefficient	23
Figure 25	Constant W/δ Strategy for Determining Compressibility Effects	24
Figure 26	Constant W/σ Strategy for Determining Compressibility Effects	25

List of Acronyms and Symbols

A_{blade}	Area of one rotor blade
A_{disk}	Area of the rotor disk
$C_{dprofile}$	Average Coefficient of drag
C_T	Coefficient of Thrust
EPR	Engine Pressure Ratio
ERiTS	Equivalent Retreating Tip Speed
ESHP	Engine Shaft Horsepower
ESHPcorr	Corrected engine shaft horsepower
FAA	Federal Aviation Administration (United States)
H-V	Height-Velocity
ICAO	International Civil Aviation Organization
M	Mach number
N_1	Gas generator speed percent rpm
N_1corr	Corrected gas generator speed
NATO	North Atlantic Treaty Organization
Nr	Rotor rpm
OEF	Operation Enduring Freedom
OEI	One Engine Inoperative
P_a	Ambient pressure
Ps	Specific excess power
P_{ssl}	Atmospheric pressure sea level, standard day
P_{t2}	Inlet total pressure at the compressor face
P_{t3}	Total pressure at the compressor exit
Q	Torque
r	Radius of rotor disk to arbitrary point on the blade
R	Rotor disk radius
RPM/rpm	Revolutions Per Minute
SFC	Specific Fuel Consumption
STO	Science and Technology Organization
T_a	Ambient Temperature
t_c	Blade loading coefficient
TGT	Turbine Gas Temperature
TGTcorr	Corrected turbine gas temperature
T_{ssl}	Temperature sea level, standard day
T_{t2}	Inlet total temperature at the compressor face

U.S.	United States
V’	Calculated climb rate
V_f	Forward flight airspeed
v_{ih}	Induced hover velocity
VRS	Vortex Ring State
V_t	True airspeed
V_v	Measured climb rate
W	Gross Weight
W_a	Mass flow
$W_a$corr	Corrected mass flow
W_f	Fuel flow
$W_f$corr	Corrected fuel flow

Symbols

δ	Pressure ratio
δ_a	Ambient pressure ratio
δ_{t2}	Total pressure ratio at the compressor face P_{t2}/ P_{ssl}
θ	Standard temperature ratio
θ_{t2}	Total temperature ratio at the compressor face T_{t2}/ T_{ssl}
μ	Advance ratio
ρ	Density
ρ_a	Ambient density
ρ_{ssl}	Ambient density at sea level, ICAO standard day
σ	Density ratio
σ_R	Rotor disk solidity ratio
Ω	Rotor angular velocity

Author Contact Information

Name:	Mr. John O'Connor
Mailing Address:	U.S. Naval Test Pilot School NAWCAD 5.1.5 22783 Cedar Point Road Patuxent River, MD 20670 UNITED STATES
Email:	john.c.oconnor@navy.mil

Name:	Mr. Jim McCue
Mailing Address:	U.S. Naval Test Pilot School 22783 Cedar Point Road Patuxent River, MD 20670 UNITED STATES
Email:	jim.mccue@navy.mil

Name:	LtCdr John Holder
Mailing Address:	KBRwyle Rotary Wing Flight Instructor USNTPS 22783 Cedar Point Road, Building 2168 NAS Patuxent River, MD 20670 UNITED STATES
Email:	john.m.holder.uk@navy.mil / john.holder@wyle.com

Name:	Mr. Bryan Carrothers
Mailing Address:	IAR-FRL 1920 Research Road Building U-61 Ottawa, Ontario KIA 0R6 CANADA
Email:	bryan.carrothers@nrc-cnrc.gc.ca

HIGH ALTITUDE ROTARY WING FLIGHT TESTING – CONSIDERATIONS IN PLANNING ROTARY WING PERFORMANCE TESTING FOR HIGH ALTITUDE OPERATIONS

1.0 INTRODUCTION

1.1 Mishaps Caused by Weight, Altitude, and Temperature Effects

The performance charts for helicopters deployed by the NATO members were generated by flight tests scoped to cover altitudes relevant to the expected mission environments. The models used to generate those graphs were well-behaved given the domain of interest.

The mission environment encountered in Afghanistan challenged the validity of the generalized data model used for the generation of the performance charts. Specifically, the atmospheric effects of temperature and pressure imposed limitations on the performance of both the engine and the rotor system. The power produced by the engine, the power required for the rotor and the change in the corresponding drag were not well-characterized at temperature and pressure extremes during the initial testing.

Mishaps occurred in OEF and during high altitude rescue operations in mountainous regions of the world. The cause factors in those mishaps pointed to three mechanisms; the effect of temperature on the engine power available limits, the effect of temperature on the compressibility effect on the rotor system, and the effect of temperature on the stall characteristics of the rotor system.

These mishaps generated concern regarding helicopter operations in heavy, high, hot/cold conditions. The performance characteristics that affect the operations are reduced power available from the engine, additional power required due to retreating blade stall, additional power required due to advancing blade compressibility, inadequate rate of climb/ turn performance (specific excess power – Ps) for turbulent mountain operations, and the possibility of inadvertent vortex ring state during mountain operations.

Helicopters will continue to operate in demanding hot and cold environments at high altitude. Efficient testing is required to provide the basis for performance chart development, which accurately reflects the expected performance in these environments. This report will discuss the parameters and the test strategies to define their boundaries.

2.0 MODEL FOR POWER AVAILABLE

2.1 Standard Limiting Factors

Two subsystems govern the performance of the aircraft. A generalized data model can be derived for both the power provided by the engine and the power required for the rotor system to produce lift and overcome the drag of the rotor system and fuselage. The engine model describes the power available at a given true airspeed, ambient pressure, and ambient temperature. The rotor and fuselage model describe the power required to hover, fly level, climb, or descend at a given airspeed, blade rotational velocity, and ambient density.

The model for power available is an engine model that accounts for losses from the inlet at a given airspeed, and the effects of temperature and pressure on the mass flow of the system. Since mass flow is directly related to

power, gas generator (N_1) speed is used as the independent variable for characterizing the available Engine Shaft Horsepower (ESHP), limiting Turbine Gas Temperature (TGT), and limiting fuel flow (W_f). The variables are corrected for temperature, pressure, and engine inlet effects to generalize the power available model. [1]

The engine performance characteristics of corrected Engine Shaft Horsepower (ESHPcorr), corrected power Turbine Gas Temperature (TGTcorr), corrected fuel flow ($W_f$corr), and Specific Fuel Consumption (SFC) are plotted as a function of corrected engine gas generator speed (N_1corr). These parametric relationships define engine performance over the range of operating conditions and are corrected to standard sea level conditions for comparison purposes.

Using these relationships and imposing the transmission limit of the aircraft (ESHP limit), the TGT limit of the engine (TGT limit), the mechanical gas generator limit (N_1 limit), and the fuel flow limit of the fuel pump (W_f limit), at a given forward flight velocity, ambient temperature and pressure; one can calculate the ESHP available for those conditions.

The first step in analysing engine power available data is to correct for inlet effects by calculating the total pressure ratio and total temperature ratio at the compressor face, δ_{t2} and θ_{t2} respectively. The graphic in Figure 1 shows notional relationships between total temperature differential and the inlet recovery pressure ratio and calibrated airspeed. Although the graphic implies an increase in both parameters with an increase in airspeed, these relationships are dependent on the location and orientation of the engine with respect to the airframe. Additionally, barriers, air particle separators, and other devices which affect airflow are often placed in front of the inlet. As a result, these relationships are unique to the aircraft and even to each engine. Testing is conducted to empirically measure and plot these relationships.

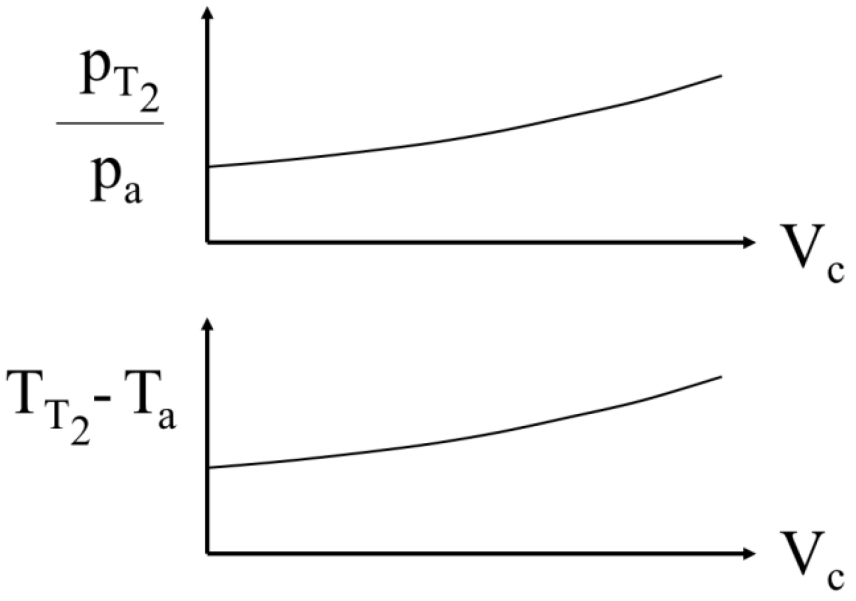

Figure 1: Inlet Recovery Relationships.

Using this relationship and each data point's ambient temperature and pressure ratio, the total pressure ratio and total temperature ratio at the compressor face for each point can be calculated by:

$$\theta_{t2} = \frac{(T_{t2} - T_a)graph + T_a}{\mathrm{T_{ssl}}}$$

$$\delta_{t2} = \frac{P_{t2}}{p_a} graph * \delta_a$$

The collected data of ESHP (torque, Q, and rotor rpm, Nr), turbine gas temperature, TGT, N_1 and fuel flow, W_f are corrected for the ambient temperature and pressure at each point:

$$ESHPcorr = \frac{ESHP}{\delta_{t2}\sqrt{\theta_{t2}}}$$

$$N_1corr = \frac{N1}{\sqrt{\theta_{t2}}}$$

$$TGTcorr = \frac{TGT}{\theta_{t2}}$$

$$\mathrm{W_fcorr} = \frac{\mathrm{W_f}}{\delta_{t2}\sqrt{\theta_{t2}}}$$

The corrected ESHP, TGT, and W_f are plotted vs. their corresponding corrected N_1. These parametric relationships define the engine's performance (Figure 2).

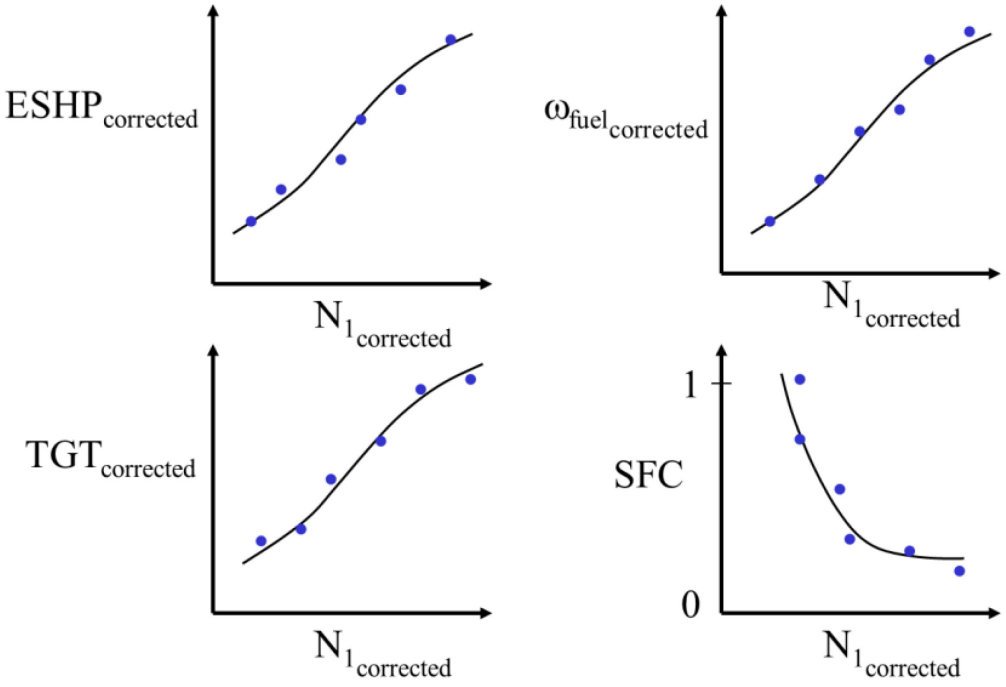

Figure 2: Generalized Engine Parameters.

The next step is to impose the corrected variables' limits and determine the corresponding corrected N_1 value. The minimum of these corrected N_1 values provides the corrected N_1 used to determine the actual ESHP available. The corrected ESHP corresponding to the minimum corrected N_1 is multiplied by the total pressure ratio and the square root of the total temperature ratio calculated for the atmospheric conditions of the applicable mission.

This method assumes the gas generator limit is a mechanical limit and that the aerodynamic conditions inside the compressor are well-behaved, that is, ambient and inlet temperature effects on compressor pressure ratio are insignificant. When this assumption is false, the pressure ratio across the compressor degrades and, since mass flow is related to power, so does the power.

A simple aerodynamic analysis of the rotor and stator in the compressor explains the effect.

In an axial flow compressor, the individual rotor blades are attached at a fixed angle. Therefore the effective angle of attack of a given blade will only vary with changes in the relative airflow. Figure 3 shows a schematic of one of the rotor blades attached circumferentially to the compressor.

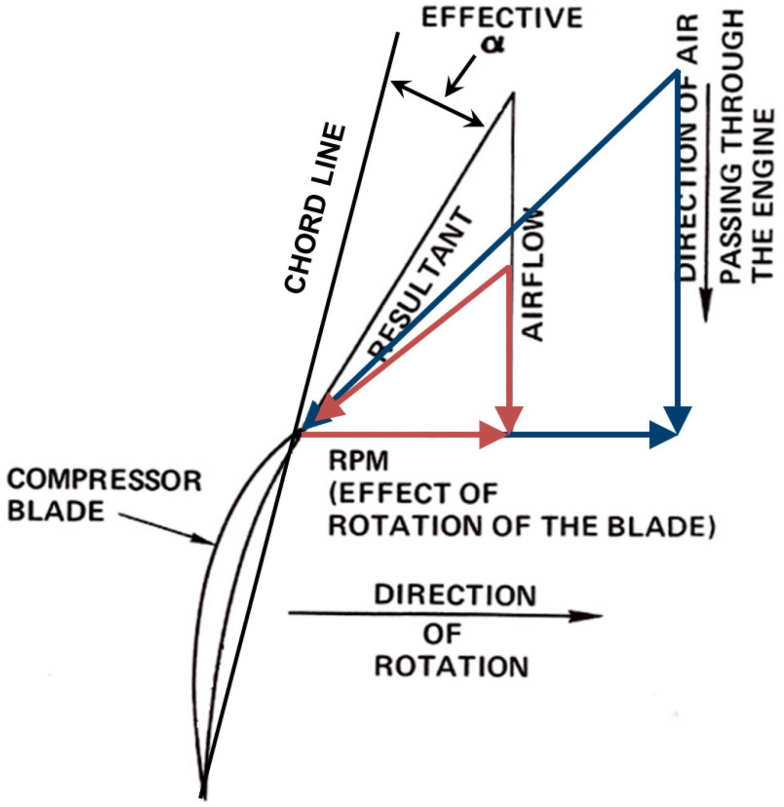

Figure 3: Blade Element Diagram of a Compressor Rotor Showing Three Different Flow Conditions.

The resultant velocity vector on the blade consists of the rpm vector and the airflow vector. The angle between the resultant velocity vector and the rotor chord line is the angle of attack. The engine is designed with variable stator blades to help control the airflow through the engine and to optimize the angle of attack at each stage. The rotor blade is an airfoil and the pressure difference created is a function of the angle of attack.

2.2 Engine Pressure Ratio (EPR) Limiting

The engine pressure ratio is the total pressure across a jet engine, measured as the ratio of the total pressure at the exit of the propelling nozzle divided by the total pressure at the entry to the compressor. Jet engines use either EPR or compressor or fan rpm as an indicator of thrust. In a turboshaft application, an examination of the total pressure ratio over the expected ambient temperature range defines the pressure ratio limit of the engine. The total pressure ratio across the compressor, P_{t3}/P_{t2}, increases linearly with an increase in the angle of attack on the compressor rotor blades (Figure 4). The relationship of pressure ratio across the compressor with angle of attack on the compressor rotor is assumed constant over the range of temperatures experienced by the engine. This angle of attack has a stall limit just like any airfoil. At this limit, the pressure ratio across the compressor will decrease rapidly as will the mass flow rate. This limit is called the surge limit. Compressor surge is characterized by a complete stoppage of flow or a flow reversal through the compressor system, or by a sharp reduction of the airflow handling ability of the engine for its operating rpm [2]. Compressor surge can damage an engine, so manufacturers will provide protection from this condition, often in the fuel control. The result is a loss of power when conditions are met that would otherwise result in surge (Figure 5).

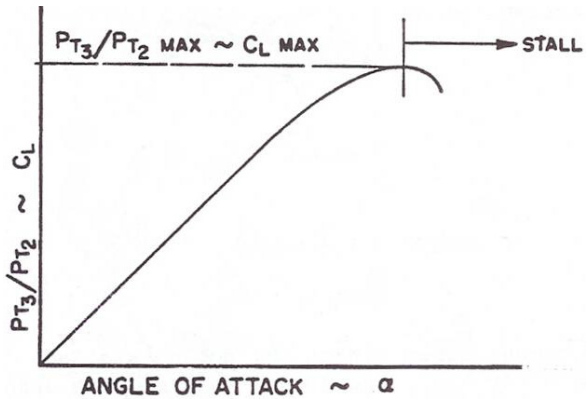

Figure 4: Pressure Ratio ~ Wing Lift Analogy.

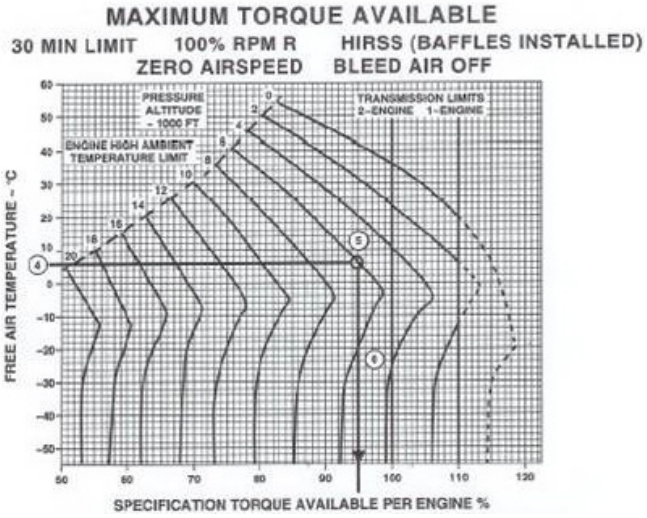

Figure 5: User's Chart Showing Loss of Torque at Temperature Extremes.

2.3 Effects of Compressor Pressure Ratio Limiting

There are a number of causes for surge. Ambient temperature conditions affect the size of both the mass flow (airflow) velocity vector and the rotational velocity vector. The mass flow, corrected for temperature and pressure ($W_a$corr) is:

$$Corrected\ Mass\ flow = \frac{Wa\sqrt{\theta}}{\delta}$$

In the summer, high altitude and hot temperatures are a concern because the static atmospheric pressure ratio, δ, is reduced. Ambient air temperature is higher than standard atmosphere so corrected mass flow will decrease with altitude, but not as much as in standard atmosphere. On a cold day, temperature is colder so the temperature

ratio, θ, is less than on a standard day. Pressure is still affected deleteriously and now corrected airflow is less than on a standard day. If this were the only effect of temperature (we assume for illustrative purposes that the rotational vector remains constant), the angle of attack of the resultant vector would increase (red vectors, Figure 3 and Figure 6). The magnitude of the rotational vector is defined by the corrected gas generator speed, which is the rotational speed of the compressor divided by the square root of the temperature ratio, θ:

$$N_{1corr} = \frac{N_1}{\sqrt{\theta}}$$

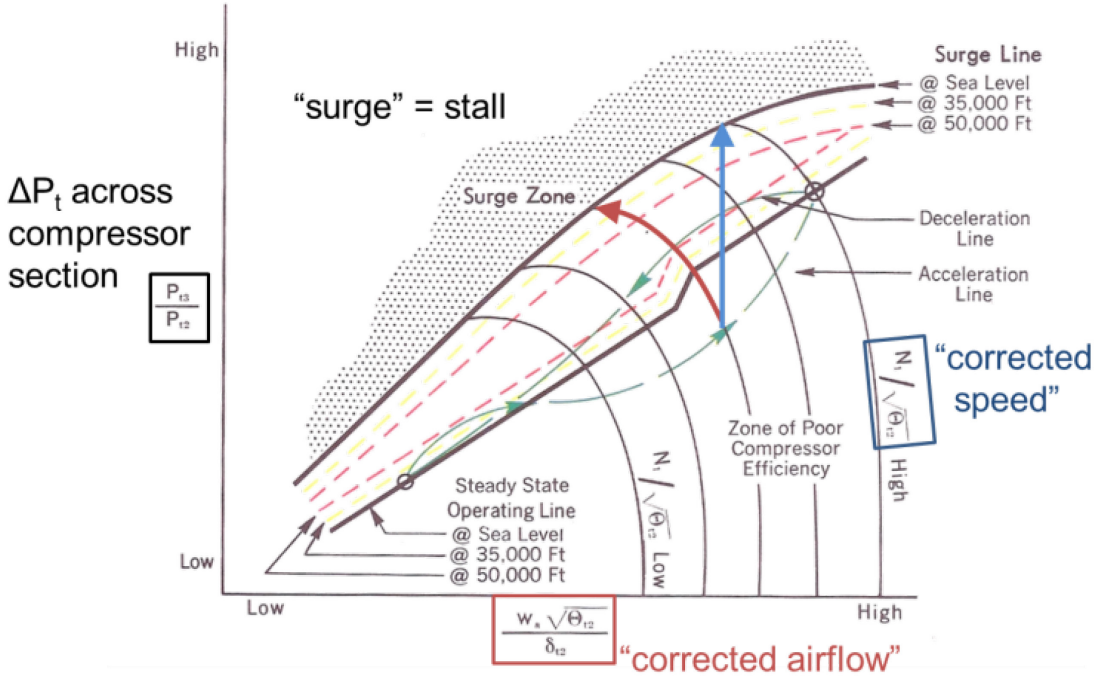

Figure 6: Engine Compressor Performance Map.

As the temperature goes down (i.e. colder than standard day condition), the corrected rotational speed gets larger. Again, for illustrative purposes, if the airflow vector remained constant, the elongation of the corrected rotational speed vector would cause the resultant angle of attack to increase (blue vectors, Figure 3 and Figure 6).

Lower temperatures affect both the corrected airflow speed and the corrected rotational speed and both of those conditions result in an increased angle of attack. The added effects can cause compressor surge (Figure 6). As power is added to the engine, the corrected compressor speed and the corrected mass flow increase until an angle of attack limit is reached and with it, a corresponding compressor pressure limit P_{t3}/P_{t2}. At this point, the compressor surges. Reynolds number effects on each compressor blade change the efficiency of the compressor as altitude increases so the angle of attack at which the blade stalls, and the corresponding compressor ratio, changes with altitude. Thus, there are different surge lines for different altitudes. The indications in the cockpit do not identify an approaching power available limit (i.e. impending surge). No predicted engine limits have been reached, yet the engine is surging and the rotor system may be drooping. Also, if bleed air powered anti-icing or cabin heat is selected ON then surge will happen sooner. If you are single engine or One Engine

Inoperative (OEI), the raw N_1 will be higher so onset of EPR limiting will happen sooner too, i.e. at warmer and lower altitudes.

The test implications are simple. The test organization must plan for high altitude and low temperature conditions in order to produce an accurate model that can predict engine performance under extreme operation conditions. However, the amount of flight test conducted is usually a compromise based on the resources available. The U.S. Federal Aviation Administration's civilian certification guidance provided in para 29.45 of Ref. [9] allows extrapolation and interpolation of flight test results using good engineering judgment. It also recognizes that traditional performance test methods have proven insufficient with modern rotorcraft designs; however, analysis is permitted if the methodology is suitable. It is believed that the methodology presented herein is suitable and would support extrapolation up to ±4,000' density altitude for hover, takeoff and landing performance and up to ±2,000' density altitude for handling qualities, Height-Velocity (H-V) and engine operating characteristics. The FAA guidance also warns against extrapolations and interpolations exceeding 10°C below or 20°C above the flight test conditions.

3.0 MODEL FOR POWER REQUIRED

3.1 Standard Model Variables

The power required model accounts for induced power, profile power (power required to drag the rotor system through rotation), the parasite power (power required to move the airframe through the air), the power for engine and transmission accessories, the power to overcome stall effects on the rotor system (retreating blade stall), and the power incurred when the blades are experiencing the effects of compressibility (Figure 7).

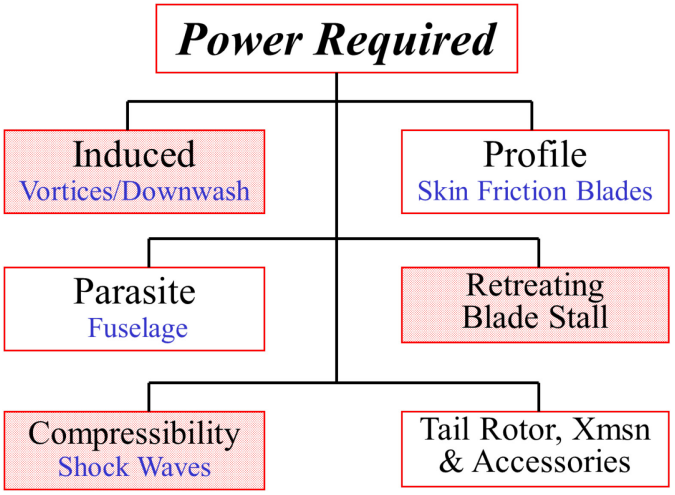

Figure 7: Power Required Elements.

The standard hover model describes the contribution of induced and profile power and is written:

$$ESHP = \sqrt{\frac{W^3}{2\rho A_{disk}}} + \frac{1}{8} C_{dprofile} \rho_a A_{disk} \sigma_R (\Omega R)^3$$

Two assumptions are made in the derivation of the model; first the effects of compressibility are insignificant and an average coefficient of drag ($C_{dprofile}$) can be used since the angle of attack will not vary significantly. The forward flight model describes the contribution of induced, profile and parasite power. In describing the parasite power, spanwise drag on the rotor blades contributes to the power required. The same assumptions made in hover are maintained in forward flight:

$$ESHP = \frac{W^2}{2\rho A_{disk} V_t} + \frac{1}{8} C_{dprofile} \rho_a A_{disk} \sigma_R (\Omega R)^3 (1 + 4.65 {V_t}^2)/(\Omega R)^2) + \frac{1}{2} \rho {V_t}^3 f$$

The two assumptions made in the derivation can break down with significant effects. In forward flight, the retreating blade can get to an angle of attack where it stalls. Compressibility of the advancing blade tip can affect both hover and forward flight. Both conditions can affect power required. Figure 8 shows the velocity and resulting lift dissymmetry in forward flight.

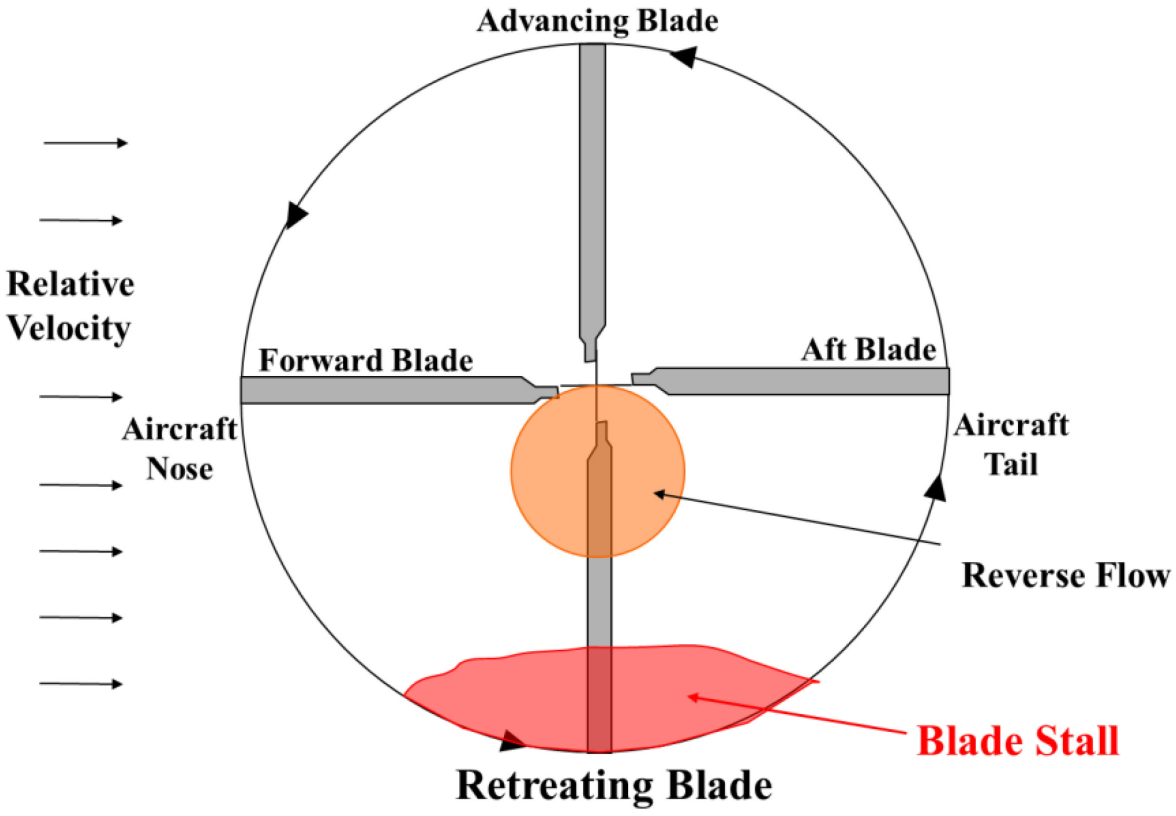

Figure 8: Dissymmetry of Lift in Blade Stall.

3.2 Blade Aerodynamics

The resultant speed on the advancing blade is equal to the sum of the blade's rotational velocity plus the helicopter's forward speed:

$$V_f + \Omega r$$

The resultant speed at any point on the retreating blade is equal to the sum of the helicopter's forward speed minus the blade's rotational velocity:

$$V_f - \Omega r$$

A section of the retreating blade is moving forward through the air when the aircraft's airspeed is faster than the component of the chordwise speed generated by the rotation of the rotor. The point at which the resulting speed is zero (forward speed is equal to the tangential speed of rotation) occurs when:

$$V_f = \Omega r$$

The proportion of the blade in reverse flow is defined as:

$$\frac{r}{R} = \frac{V_f}{\Omega R}$$

Where the advance ratio, μ, is defined as:

$$\frac{V_f}{\Omega R} = \mu$$

3.3 Blade Stall

As the forward airspeed increases, the region of the retreating blade that is in reverse flow increases and the region of the blade that can produce lift decreases. If lift (L) on the blade is a function of angle of attack (α), density (ρ), velocity, and the area of the blade (A) that is not in reverse flow such that:

$$L \text{ is proportional to } (\alpha * \rho * V^2 * A)$$

Then to maintain balanced lift, as blade area decreases, angle of attack must increase. The condition is aggravated with increased forward cyclic as the demand for forward tilt of the tip path plane increases the lift requirement on the retreating blade. The retreating blade will stall at some point. Prior to this point, the coefficient of drag will increase rapidly and the assumption made in the derivation of the model that the coefficient of drag will remain relatively constant and well-behaved will be invalid. The profile drag will rise rapidly. The power required will increase in a manner not accounted for in the model. Consequently, each blade will move in and out of stall as it rotates and the stresses imparted on the pitch change links and other components can cause the loss of the aircraft. This is normally accounted for in the V_{ne} changes of the aircraft with respect to increasing altitudes and decreasing temperatures, but non-standard hot/high conditions are not normally considered, increasing the risk of unexpected retreating blade stall.

3.4 Compressibility at the Blade Tips

Flight conditions at high altitude and cold temperatures are a concern because they provide the required conditions for compressibility effects. Compressibility can affect the power required in both hover and forward flight. As the speed of the tip of the advancing blade approaches the local speed of sound, the air is compressed and a shock wave begins to form. Normally in a hover the blade is traveling at a Mach number of 0.6 to 0.7:

$$M = \frac{V_t}{(Speed\ of\ sound)}$$

$$Speed\ of\ Sound(kts) = 38.9\sqrt{T_a(K°)}$$

As the temperature decreases, the Mach number for the same rotational speed (rpm) increases. Again, in forward flight, the resultant speed on the advancing blade is equal to the sum of the blade's rotational velocity plus the helicopter's forward speed. As a result, the Mach number of the advancing blade is greater in forward flight than in a hover at the same temperature. Figure 9 shows the dissymmetry of lift caused by compressibility effects on the advancing blade in forward flight.

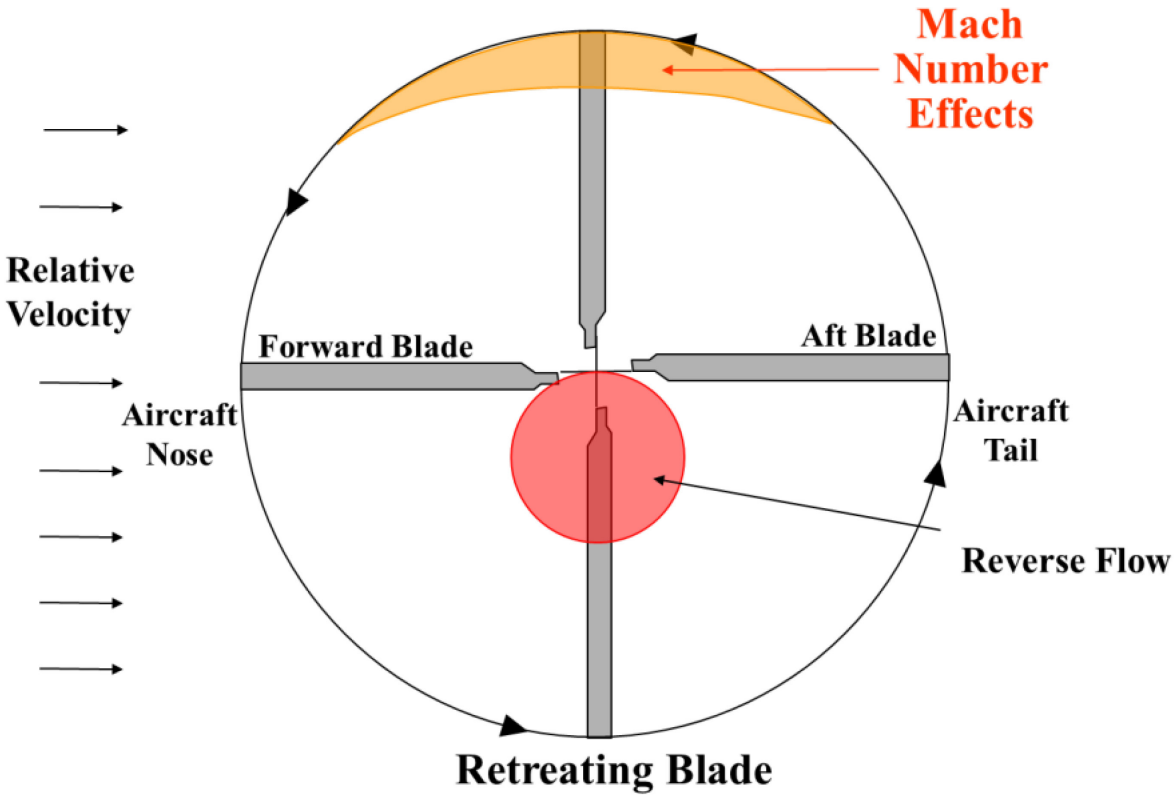

Figure 9: Dissymmetry of Lift from Compressibility Effects.

The critical Mach number is the Mach of the freestream at which a portion of the blade is at Mach 1 or the speed of sound. At freestream Mach numbers greater than this, a shock wave forms and with it, an associated drag rise and increase in power required, Figure 10, Figure 11(a) and Figure 11(b).

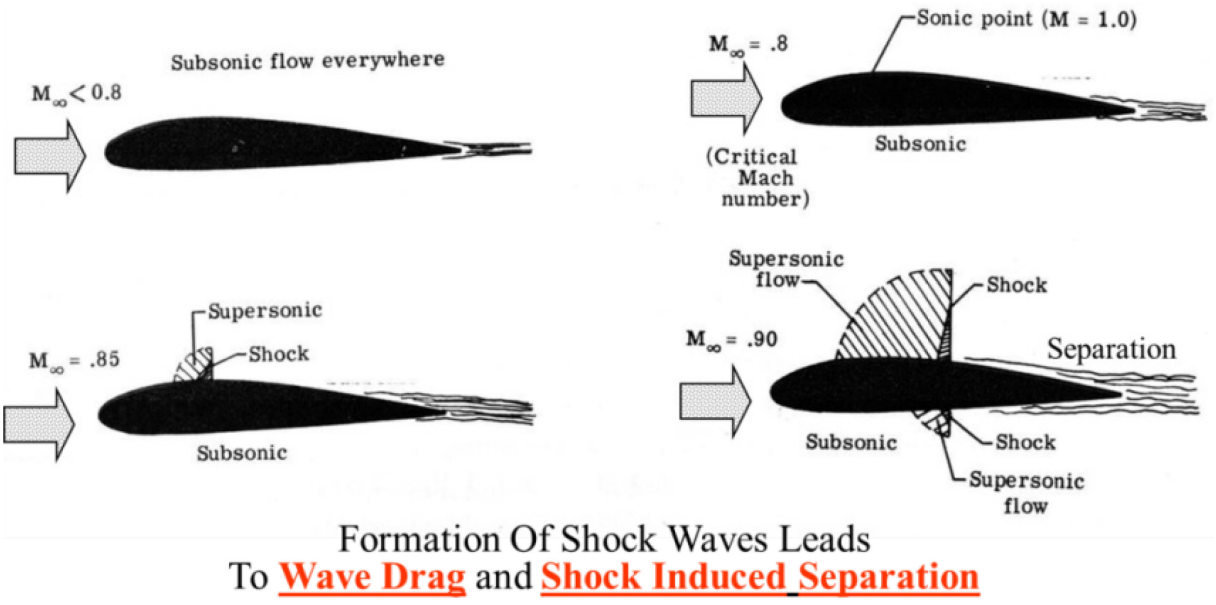

Figure 10: Formation of Shock Waves.

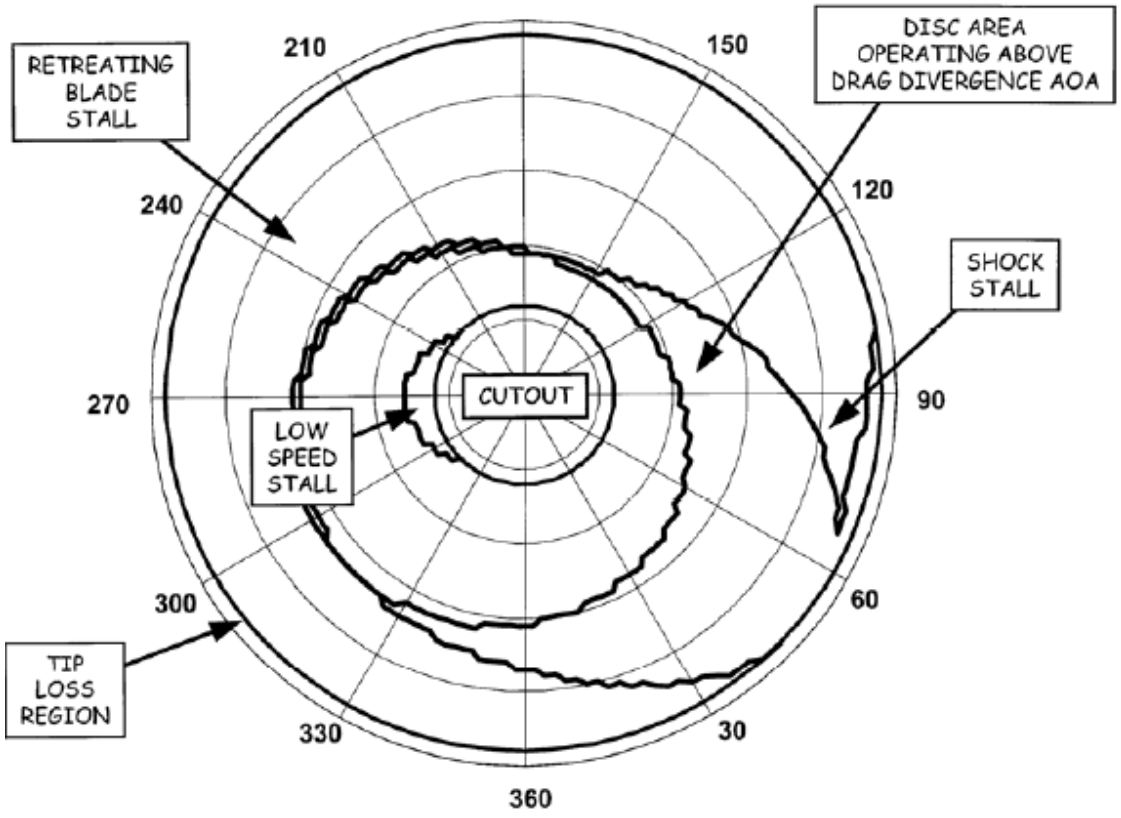

Figure 11(a): Rotor Map-Simultaneous Stall and Compressibility Conditions in Forward Flight (counter-clockwise blade rotation, 120 knots, 20.3 degrees collective pitch, 104 KN thrust) [8].

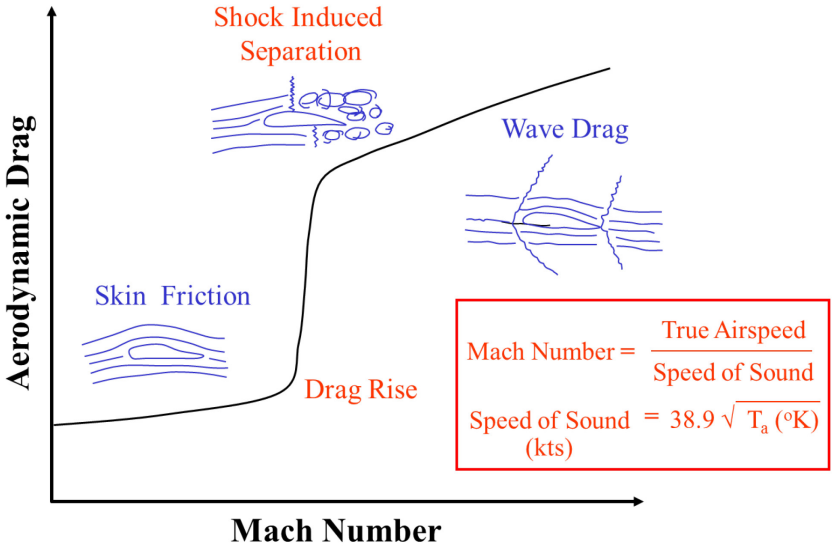

Figure 11(b): Shock-Induced Drag Rise.

4.0 INFLUENCES OF WEIGHT, TEMPERATURE, AND ALTITUDE ON POWER

4.1 Hover: Influences of Weight and Temperature, Hot and Cold

In hover, the angle of attack is low enough that compressibility effects won't occur until the blade rotation speed and ambient temperature produce a Mach number around 0.8. The Mach number at which the shock wave forms is a function of the angle of attack and the tip sweep/design of the blade. In a hover, the shock wave forms on the top of the blade. However, in forward flight, as the advancing blade decreases pitch, it is possible for the angle of attack on the advancing blade to attain a negative value momentarily and for the shock to form on the bottom of the blade. The local Mach number does not have to equal "1" for the shock wave to form in either case (Figure 12) and the model does not describe the drag associated with it.

Figure 13 through Figure 15 graphically depict the notional effects of temperature on power available and power required in hover. Power required in hover increases directly with weight (Figure 13). Although density is in the induced and profile term of the hover equation, a decrease in density (with an increase in temperature) has a beneficial effect to profile power required but a negative effect to the induced power required. The overall effect is an increase in power required (Figure 14). As the temperature decreases, the local speed of sound decreases and the effect of compressibility can be realized on all blades simultaneously. If we no longer assume that the angle of attack is low enough that compressibility effects will not occur, the effect is a substantial increase in power required. Recall that the lower temperature also affects the engine pressure ratio so the resulting power available is also less than on a standard day (Figure 15).

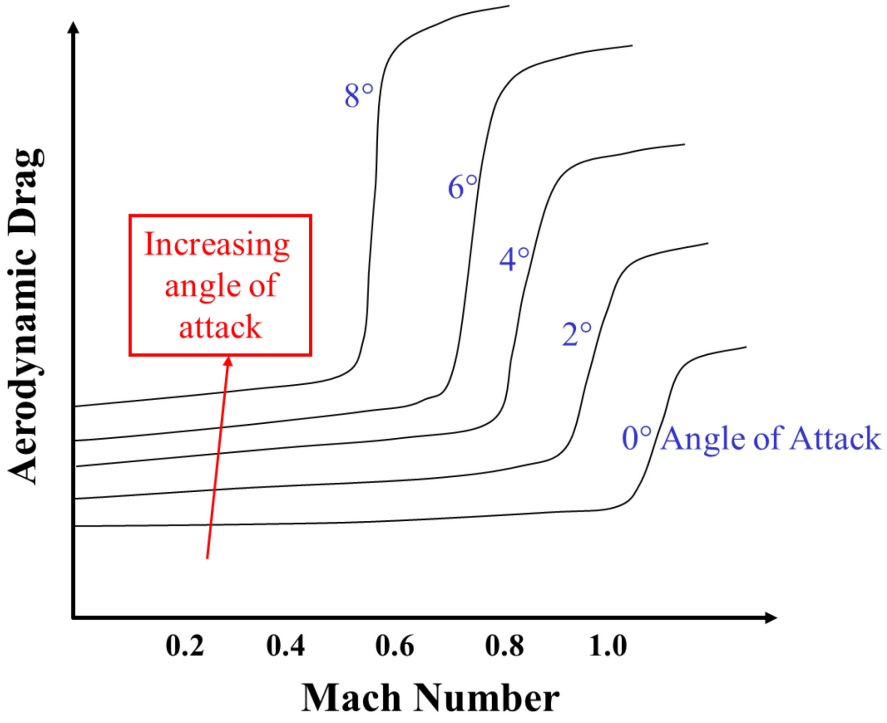

Figure 12: Aerodynamic Drag as a Function of Mach and Angle of Attack (Subsonic Airfoil).

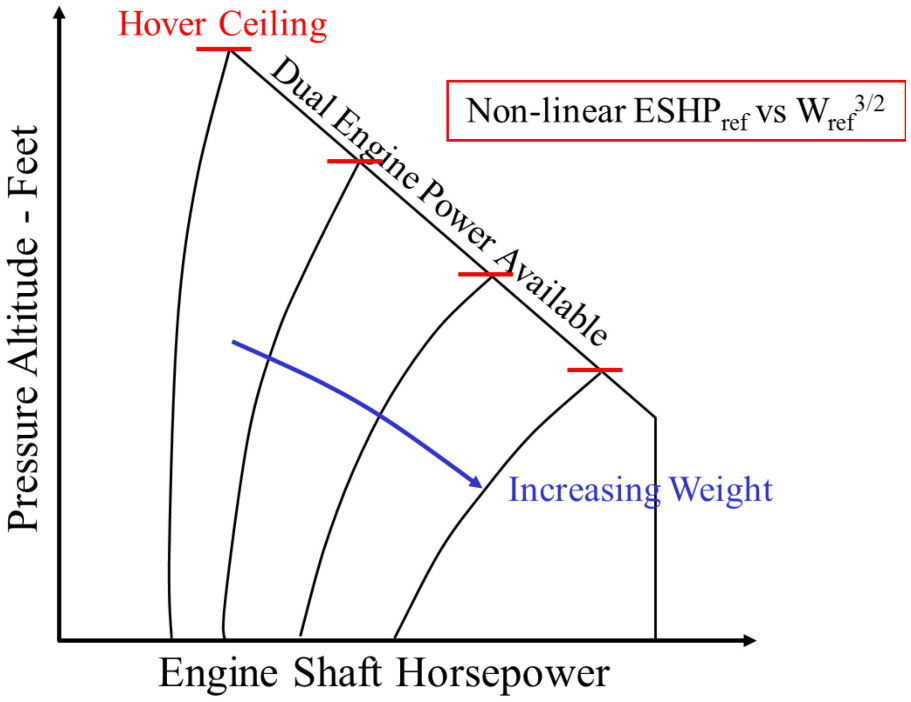

Figure 13: Increase in Hover Power Required and Power Available with an Increase in Weight.

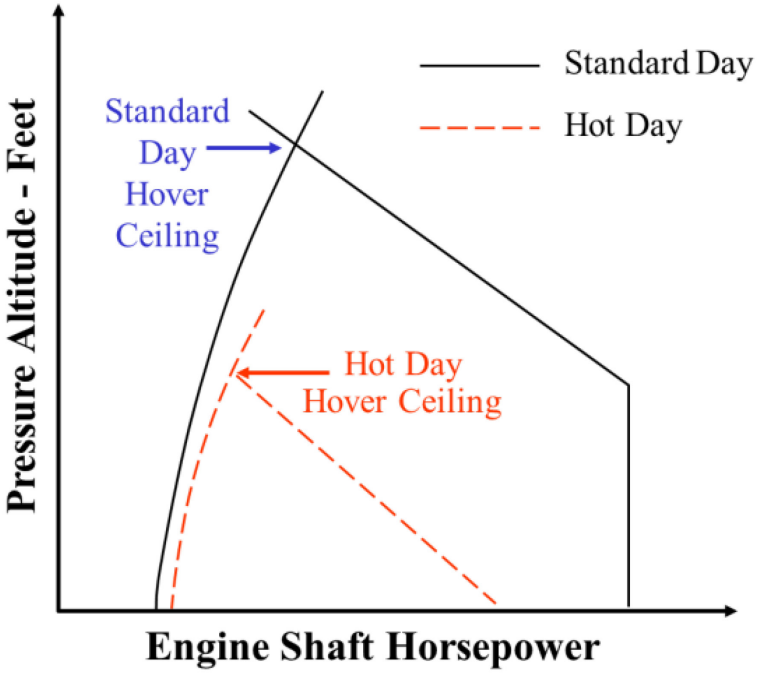

Figure 14: Effect of Temperature on Hover Power Available and Power Required – No Compressibility Effect.

Under extreme cold, compressibility affects will increase power to hover!

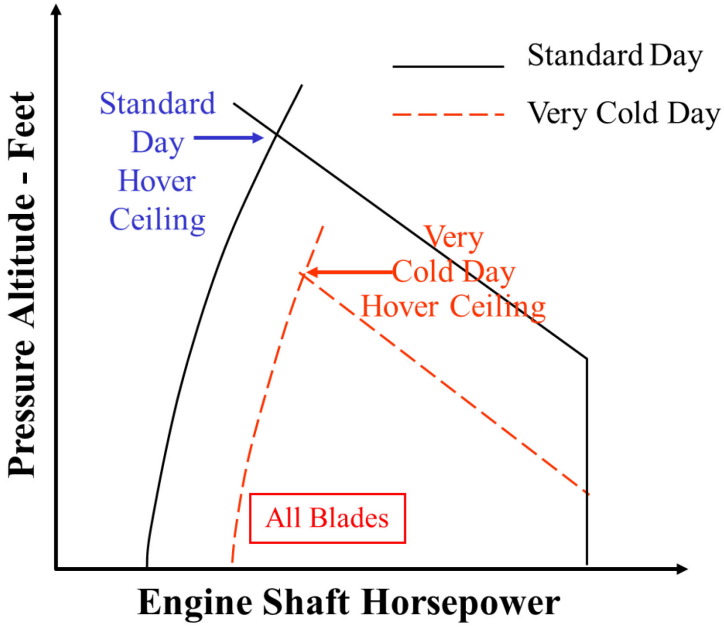

Figure 15: Effect of Temperature on Hover Power Available and Power Required – With Compressibility Effect.

4.2 Forward Flight: Influences of Weight, Blade Stall, and Compressibility

Figure 16 through Figure 19 graphically depict the notional effects of temperature on power available and power required in forward flight. Power required in forward flight increases directly with weight (Figure 16). Density is in the induced, profile, and parasite terms of the forward flight equation. A decrease in density (with an increase in temperature) has a beneficial effect to both profile and parasite power required but a negative effect to the induced power required. However, the induced power required decreases with forward speed so the overall effect is an increase in power required at low speeds and a decrease in power required at high speeds (Figure 17). If the temperature is high enough, the decreasing density sets up a requirement for more pitch on the retreating blade to generate the same lift. More pitch results in a blade stall condition (Figure 18). As the temperature gets lower, the local speed of sound decreases and the effect of compressibility can be realized on the advancing blade. If the assumption about the effect of compressibility is vacated, the effect is a substantial increase in power required. Again, the lower temperature limits the engine pressure ratio and the power available is less than on a standard day (Figure 19).

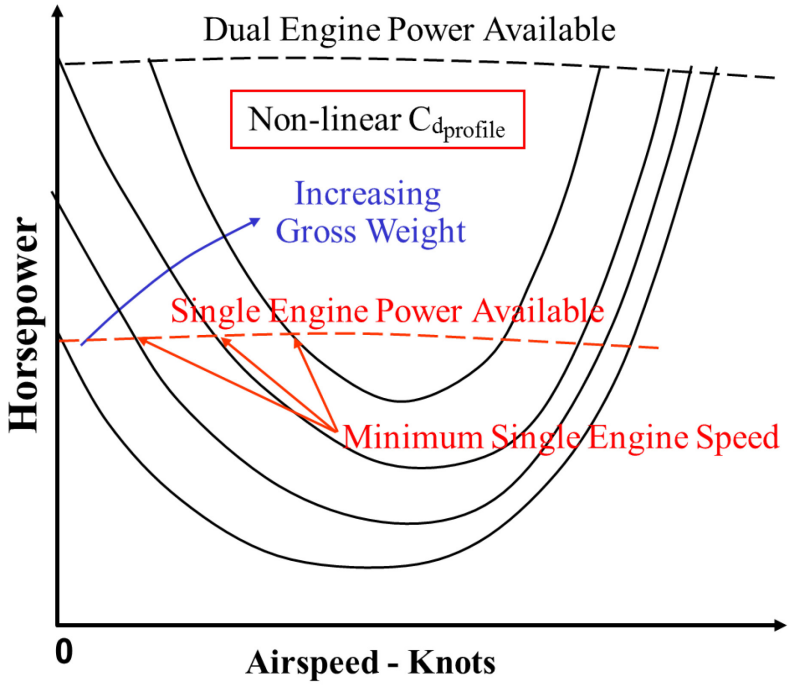

Figure 16: Increase in Power Required with Increased Weight (Forward Flight).

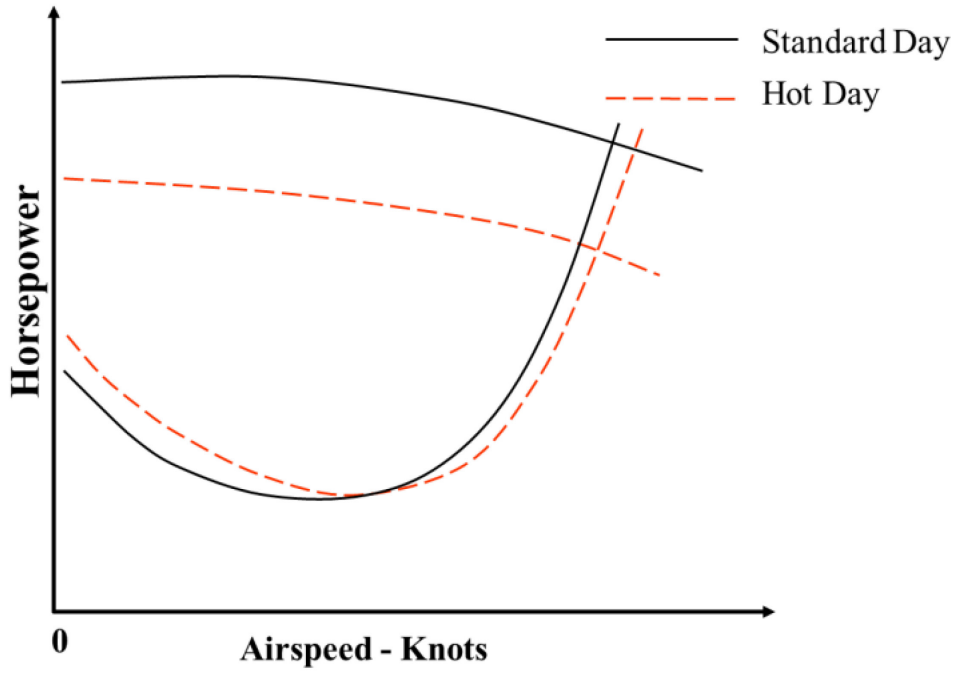

Figure 17: Effect of High Temperature (Decreased Density) on Power Required and Available (Forward Flight).

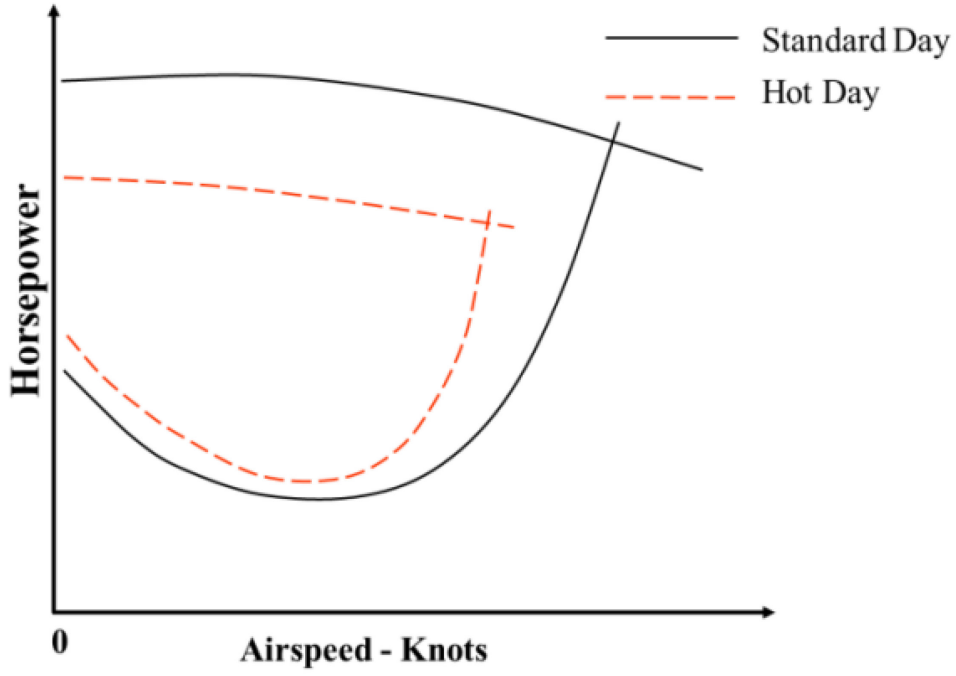

Figure 18: Effect of High Temperature (Decreased Density) with Blade Stall on Power Required (Forward Flight).

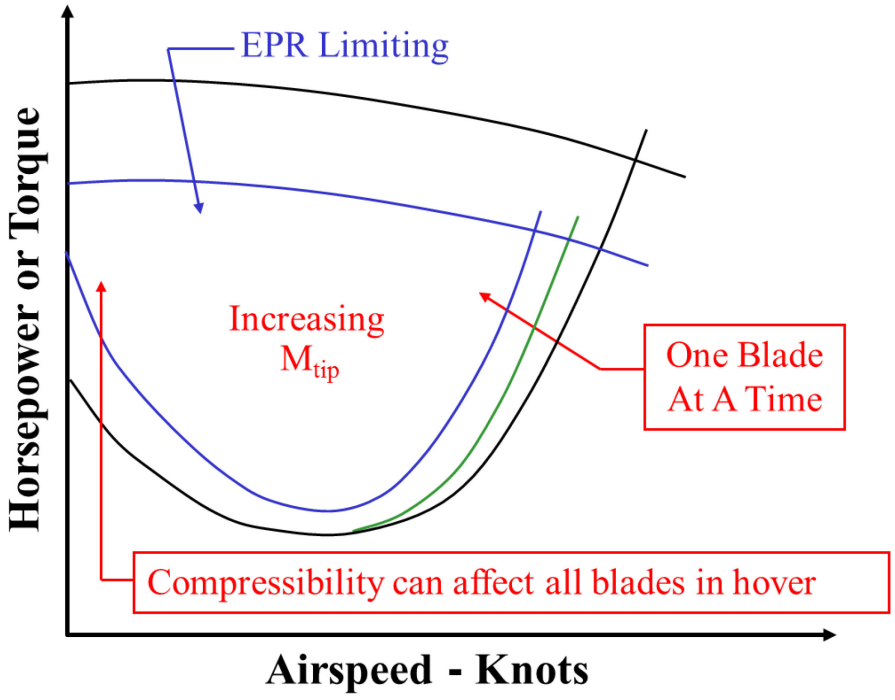

Figure 19: Effect of Low Temperature (Compressibility) on Power Required and Pressure Ratio Limiting on Power Available (Forward Flight).

4.3 Climb/Descent: Influences of Blade Stall on Climb/Descent Speeds

Climb performance in ft/sec can be calculated using the excess energy or difference between power required and power available for level flight divided by the gross weight:

$$V' = \frac{ESHP_{avail} - ESHP_{reqd}}{W} * 33000$$

In a stabilized climb the mass flow rate through the rotor is greater than in forward flight so the induced velocity and the corresponding induced power is less in a climb. As airspeed increases, this benefit decreases along with the induced power contribution to the total power required. Also, this calculated climb rate assumes that the parasite drag of the fuselage is the same in climb as it is in level flight. This assumption is not valid since the angle of attack on the fuselage changes in the climb, the faceplate drag also changes and likely increases so the power required increases and overwhelms any benefit from lower induced power. As a result, the measured climb rate is lower than the calculated rate. Mountainous ops require that the aircraft have sufficient excess power to counter significant downdrafts. Downdrafts of 30 ft/sec or 1800 fpm are not uncommon. Blade stall and compressibility effects reduce excess power and corresponding calculated rate of climb and can drive the maximum rate of climb, minimum rate of descent, and best glide airspeeds to a slower than predicted value. The result can limit the helicopter's ability to counter strong downdrafts and sets up the conditions conducive for vortex ring state on the main rotor.

4.4 Maneuvering Flight: Influences of Blade Stall and Compressibility

Excess energy can also be used to define the maneuvering envelope as a function of altitude and airspeed for a given physical configuration. Figure 20 shows an energy management diagram for an unnamed helicopter. The lines of constant specific excess power, Ps, are depicted on a graph ranging altitude and airspeed. The energy management curves are an engineering transition of the power required and power available curves. Once the power available and power required have been determined for level flight conditions, using either the W/δ or W/σ approach, specific excess power can be calculated by subtracting power required from power available and dividing by the weight of the aircraft:

$$\text{Ps(fpm)} = \frac{ESHP_{avail} - ESHP_{reqd}}{W} * 33000$$

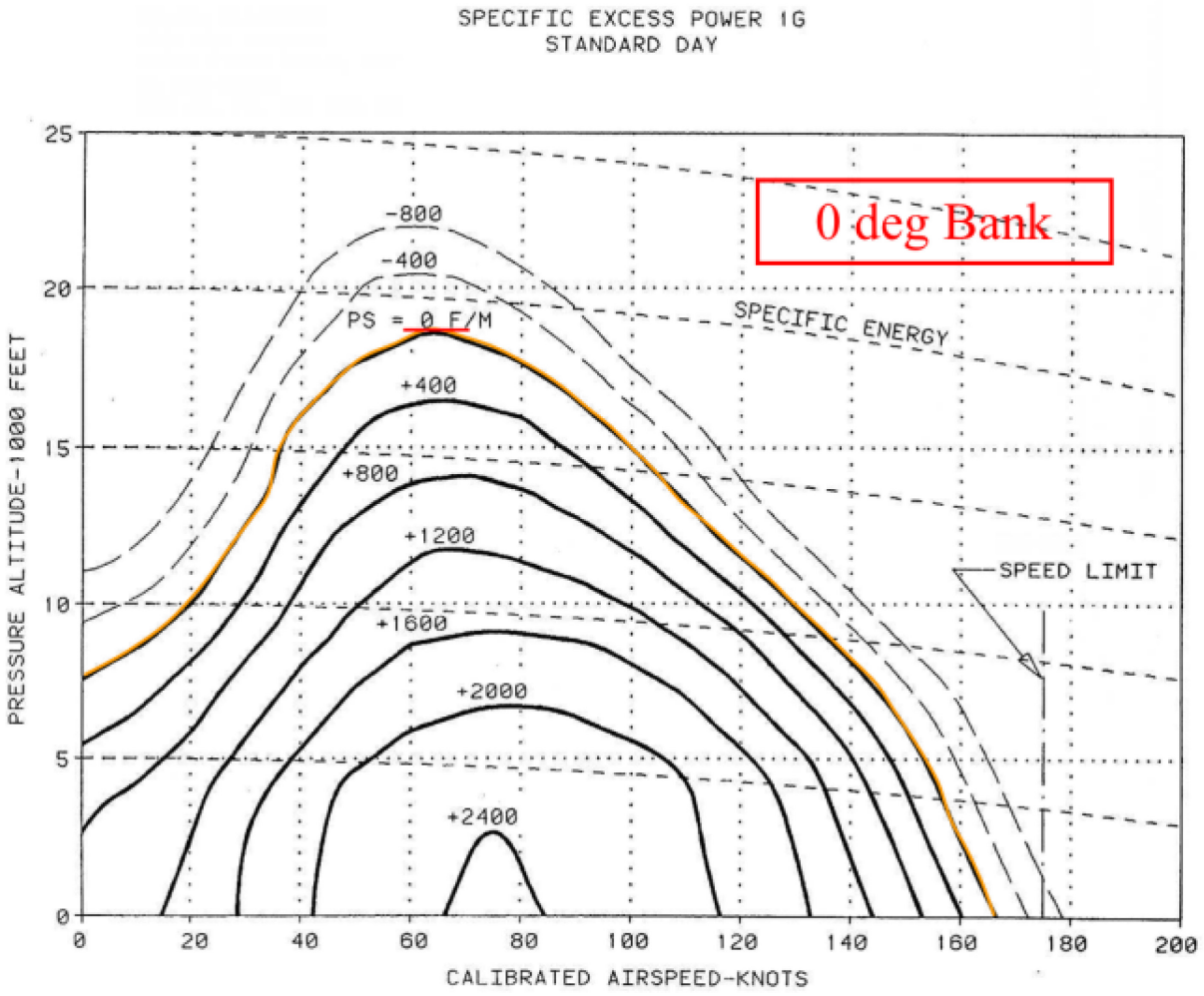

Figure 20: Energy Management Diagram-Zero Angle of Bank.

Fixed wing aircraft use a level acceleration technique where a timed, level acceleration at maximum power is conducted at different altitudes. This is impractical in a helicopter since the thrust vector is tilted forward using the tip path plane which would be constantly changing as the aircraft accelerated to maintain level flight.

The resulting variations in fuselage pitch attitude greatly affect the parasite drag of the aircraft so results are likely inconsistent. Each Ps line provides the rate of climb at an altitude and airspeed at zero angle of bank. The Ps line corresponding to zero rate of climb provides the maximum altitude at a set airspeed. The operator can use the graph to determine his minimum and maximum airspeed at a given altitude and his max rate of climb and best climb speed at a given altitude. As weight increases, Ps decreases. For maneuvering flight, maintaining level flight at a given angle of bank requires an increased normal load on the aircraft. This has the same effect on Ps at increasing the weight of the aircraft. Thus, at 45 degrees angle of bank, the maximum altitude at which the aircraft will maintain altitude (Ps = 0) is lower (Figure 21). The curves do not account for the increase in parasitic drag associated with the change in pitch attitude in a turn so a spot check of the curves at higher turn rates is warranted.

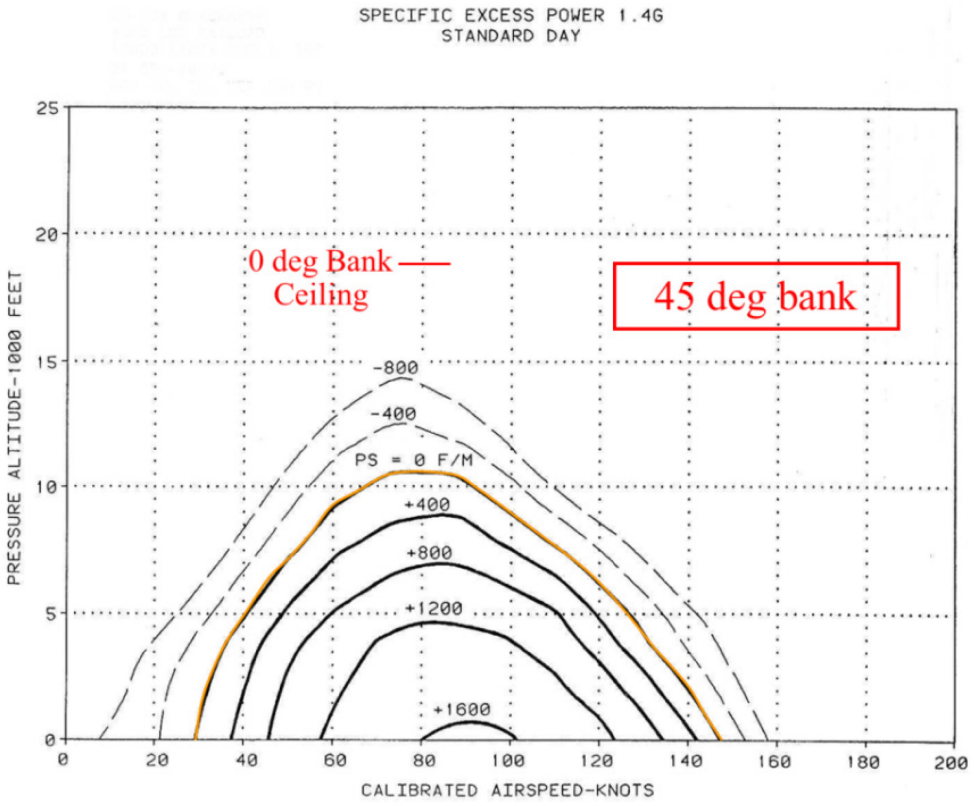

Figure 21: Energy Management Diagram-45 Degree Angle of Bank.

Energy management diagrams can be generated to provide the user with maneuvering limits for different altitudes (Figure 22 and Figure 23).

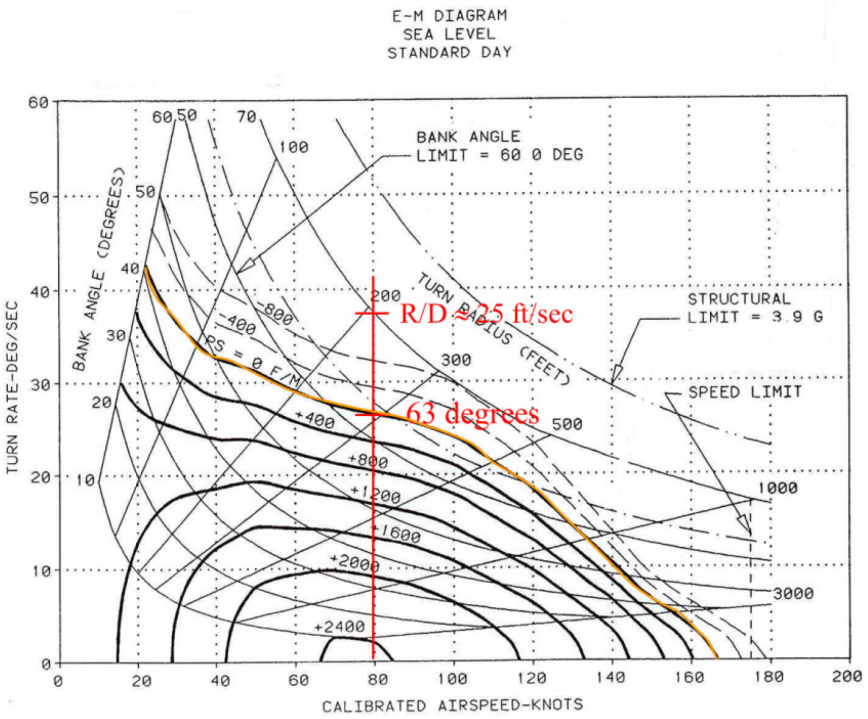

Figure 22: E-M Diagram, Sea Level, Standard Day.

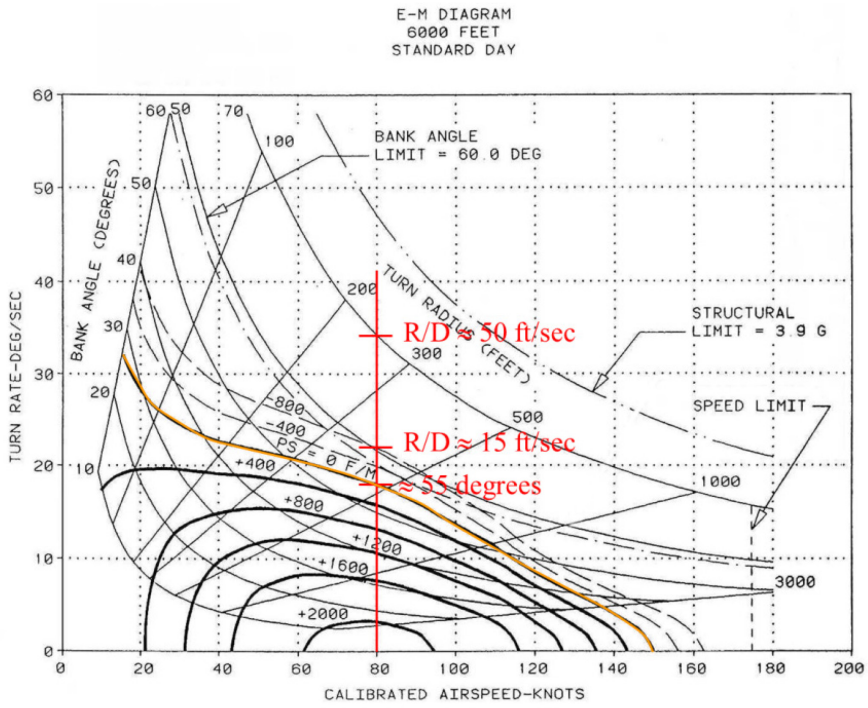

Figure 23: E-M Diagram, 6K Feet, Standard Day.

Figure 22 is an E-M diagram for a notional helicopter at sea level, standard day. Using the diagram, at 80 knots the best turn rate in a level turn (where Ps equals zero) is 27 deg/sec and 63 deg angle of bank, yielding a turn radius of 300 feet. If the aircraft is over-banked by ten degrees, the aircraft quickly picks up a rate of descent of 25 ft/sec. If the helicopter is at six thousand feet, standard day (Figure 23), the best turn rate in a level turn is 18 deg/sec at approximately 80 knots and 55 degrees where Ps equals zero, yielding a turn radius of almost 500 feet. If the aircraft is over-banked by five degrees, the aircraft quickly picks up a rate of descent of 15 ft/sec. If the pilot increases to 70 degrees, the descent rate reaches 50 ft/sec.

One can see that the aircraft maneuvering performance is greatly affected by altitude and the operators must be familiar with the effects and limitations. Energy management diagrams must be provided for high altitude conditions. These diagrams need to incorporate the test results of compressibility and blade stall and so the test planning process needs to be informed by these requirements.

5.0 VORTEX RING STATE

5.1 Vortex Ring State Scenario

There are a range of airspeeds and descent rates over which a helicopter will recirculate its rotor wake and fail to generate effective lift. This phenomenon is usually encountered during a descent at slow airspeed, when the velocity tangent to the rotor disk is small compared to the upward velocity of the air perpendicular to the rotor disk. When collective pitch is applied to arrest the rate of descent, the circulation of the rotor downwash increases creating vertical rings of inflow and outflow, the rotor head does not produce the anticipated lift, and the aircraft's rate of descent increases. A number of criteria to define the boundaries of the phenomena have been proposed in the past. Among them are region of roughness, thrust or torque fluctuation, mean thrust reduction, zero velocity of tip vortices, blade-flapping fluctuation, wake breakdown, heave stability, and roll stability [5].

5.2 Vortex Ring State Parameters

There are many methods for predicting the boundaries created by the combination of rate of descent and forward airspeed. Ref. [3] presents many of these. Most are resolved into a combination of horizontal velocity, and vertical velocity, V_v, both normalized by the induced velocity at the rotor in a hover, v_{ih}. There is a high probability of encountering vortex ring state when the tangential velocity is small and the perpendicular velocity is large. Xin and Gao [4] found that torque fluctuations occurred when V_v/v_{ih} was -0.28. If we use this conservative boundary, we can see how we can analytically determine the vertical velocity boundary based on weight, disk area and density:

$$\frac{V_v}{v_{ih}} \leq -0.28$$

$$v_{ih} = \sqrt{\frac{W}{2\rho A_{disk}}}$$

If this boundary were plotted in terms of dimensional values, it would differ for varying atmospheric conditions (e.g., high altitude and cold temperature vice high altitude and hot). This effect is caused by the impact of air density on induced velocity. For example, as density increases for the same gross weight, v_{ih} decreases so the

vertical velocity must decrease to remain outside the boundary. This test team should therefore expect the onset of VRS at lower rates of descent then when operating in sea level conditions.

It is important to notice that this and other analytical VRS boundaries present an overly simplified view of the conditions that are conducive to VRS. In fact, the formation of VRS is a flight-path dependent phenomenon. This is to say that the onset of VRS is not only dependent on whether the instantaneous flight condition falls inside some VRS boundary; rather, it is also affected by the temporal evolution of the maneuver. For this reason, the manner in which VRS is encountered (and the way in which recovery is effected) must be tested dynamically as the aircraft maneuvers in an operationally relevant manner.

5.3 Vortex Ring State Testing

A test approach used on the V-22 to define the VRS boundaries, first statically then dynamically, while characterizing the aircraft's controllability and investigating recovery techniques is well-documented in Ref. [6] and Ref. [7].

6.0 BLADE STALL TESTING

6.1 Blade Loading Coefficient

There are two analytical methods that the tester can use to determine a test strategy to find the blade stall boundary. One uses a blade loading coefficient, t_c, which is the thrust coefficient divided by the solidity ratio of the rotor disk, σ_R. The other determines the Equivalent Retreating Tip Speed (ERiTS). Both define the boundary by setting and incrementing the test conditions until stall is detected. The dynamic components on the rotor system are instrumented to look for cyclical changes in stresses on the dynamic components corresponding to stress loading and unloading caused by retreating blade stall.

The blade loading coefficient is defined:

$$t_C = \frac{2C_T}{\sigma_R}$$

$$C_T = \frac{W}{\rho A_{disk}(\Omega R_{test})^2}$$

$$\sigma_R = \frac{A_{blades}}{A_{disk}}$$

$$t_C = \frac{2n_Z W}{\rho A_{blades}(\Omega R_{test})^2}$$

The blade loading coefficient is a function of weight, normal acceleration, air density, blade area, and rotor rpm. As the advanced ratio increases with forward airspeed, the thrust loading coefficient at which stall occurs decreases (Figure 24). As density decreases, the blade loading coefficient increases and the forward speed at which stall occurs decreases. If the rotor rpm is increased, the blade loading coefficient decreases and the forward speed at which stall occurs increases.

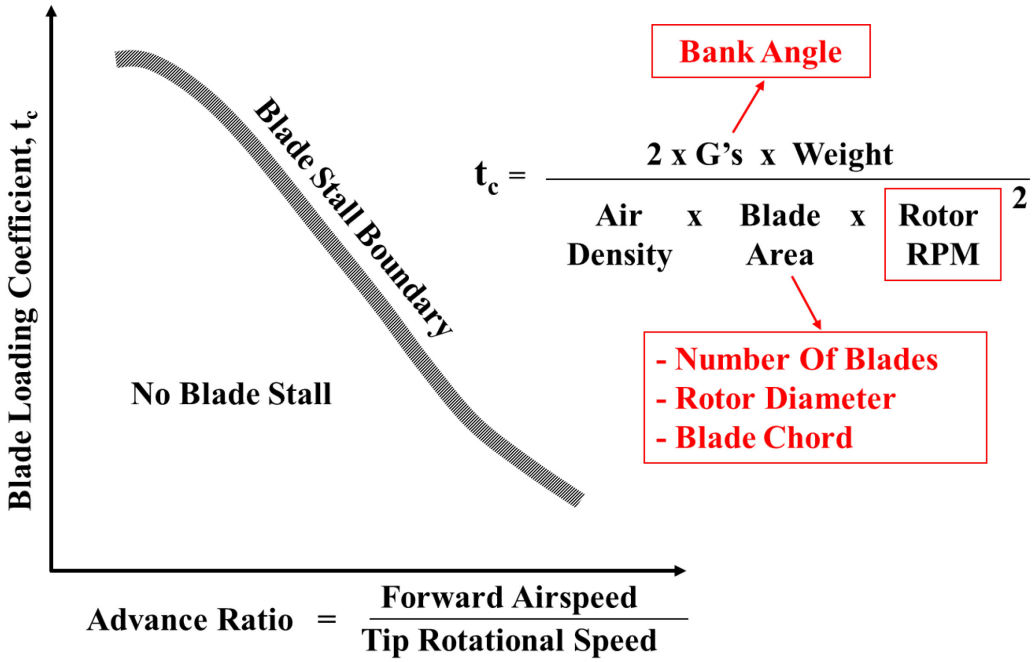

Figure 24: Blade Loading Coefficient.

Test organizations can vary airspeed, referred weight (W/σ) and rotor rpm to define where the blade stall boundary occurs. Once this boundary is known, it can be used to predict the boundary and determine the effect on power required.

6.2 Equivalent Retreating Tip Speed (ERiTS)

The ERiTS method uses an approach similar to one used to generalize the stall speed of fixed-wing aircraft. A standard mission gross weight is chosen. Again, the test team varies airspeed, referred weight, and rotor rpm. When a structural indication of blade stall occurs, the equation below can be satisfied:

$$ERiTS = (\Omega R - V_f)\sqrt{\frac{W_{std}\rho_a}{W_{test}\rho_{ssl}}}$$

Given a mission weight, altitude, and rotor rpm, an operator can determine the stall limit of the aircraft and determine the total power required for the limiting case.

7.0 COMPRESSIBILITY

7.1 A Mention of Referred Weight, Referred True Airspeed and Referred Rotor RPM

As mentioned previously, the aircraft's power required may be limited by compressibility effects. If rotor rpm is kept constant throughout the test and set at the normal operational speed, then mission-relatable referred weight is a function of weight and density at that operational rotor rpm. The W/σ method does not easily permit

investigation of changes in tip Mach number; therefore errors could arise if using results for predicting performance in very different temperature conditions. Operationally, the aircraft could be at vastly different actual weights but at the same density-based referred weight while at greatly different altitudes.

There are two strategies to capture compressibility effects during testing. A constant referred weight using weight divided by pressure ratio, δ, and vary the rotor rpm over the range allowed for the helicopter. The test objective is to gather power required at one W/δ, and more than one referred rotor rpm, rpm/$\theta^{1/2}$. The result of the data analysis is a family of referred rpm curves providing referred power required, ESHP/ $\delta * \theta^{1/2}$, as a function of referred airspeed, $V_t(\Omega R)_{std}/(\Omega R)_{test}$, for one W/$\delta$ (Figure 25).

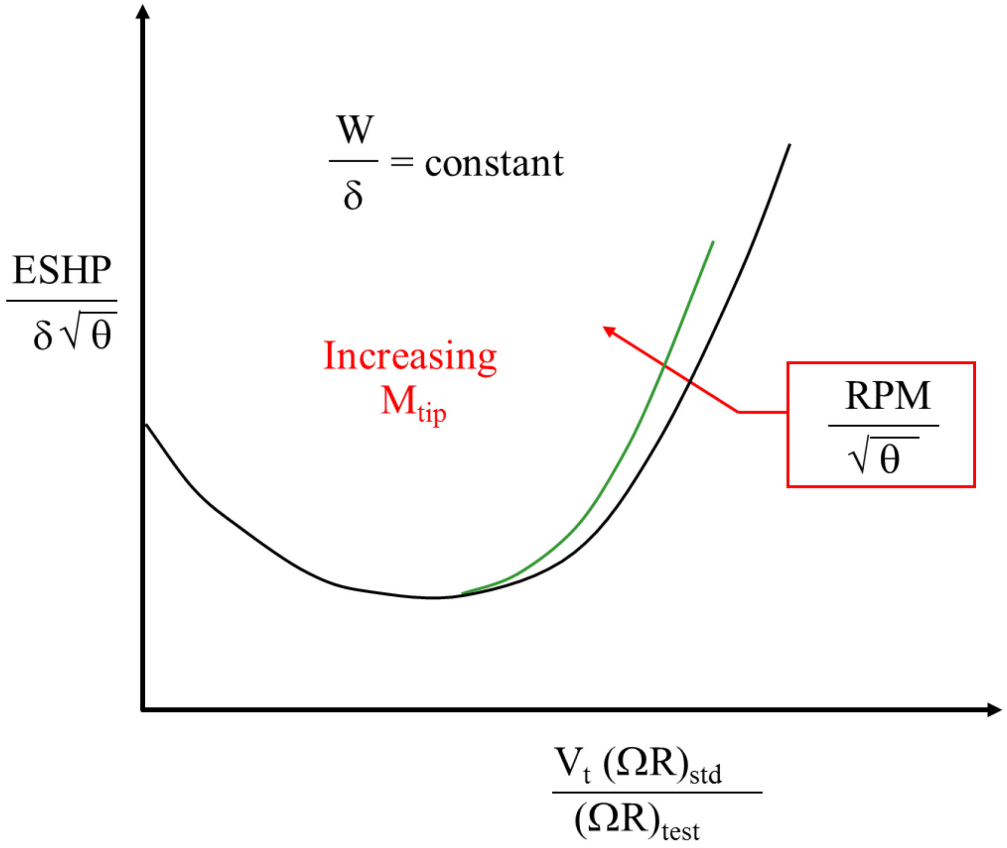

Figure 25: Constant W/δ Strategy for Determining Compressibility Effects.

In many helicopters, the rpm cannot be varied greatly so a constant W/σ method can be used with the rotor rpm set at the operational rotor rpm. In order to obtain data with the effects of compressibility, the same referred weight must be flown at altitudes yielding different combinations of weight and density ratio. Much like varying the rpm to maintain a constant referred rpm, altitudes are chosen to vary the inverse of the square root of the atmospheric temperature ratio, θ, at the constant rpm. This approach is harder to scope but the result is a family of referred rpm curves providing referred power required, ESHP/ $\delta * \theta^{1/2}$, as a function of referred airspeed, V/rpm, for one W/σ (Figure 26).

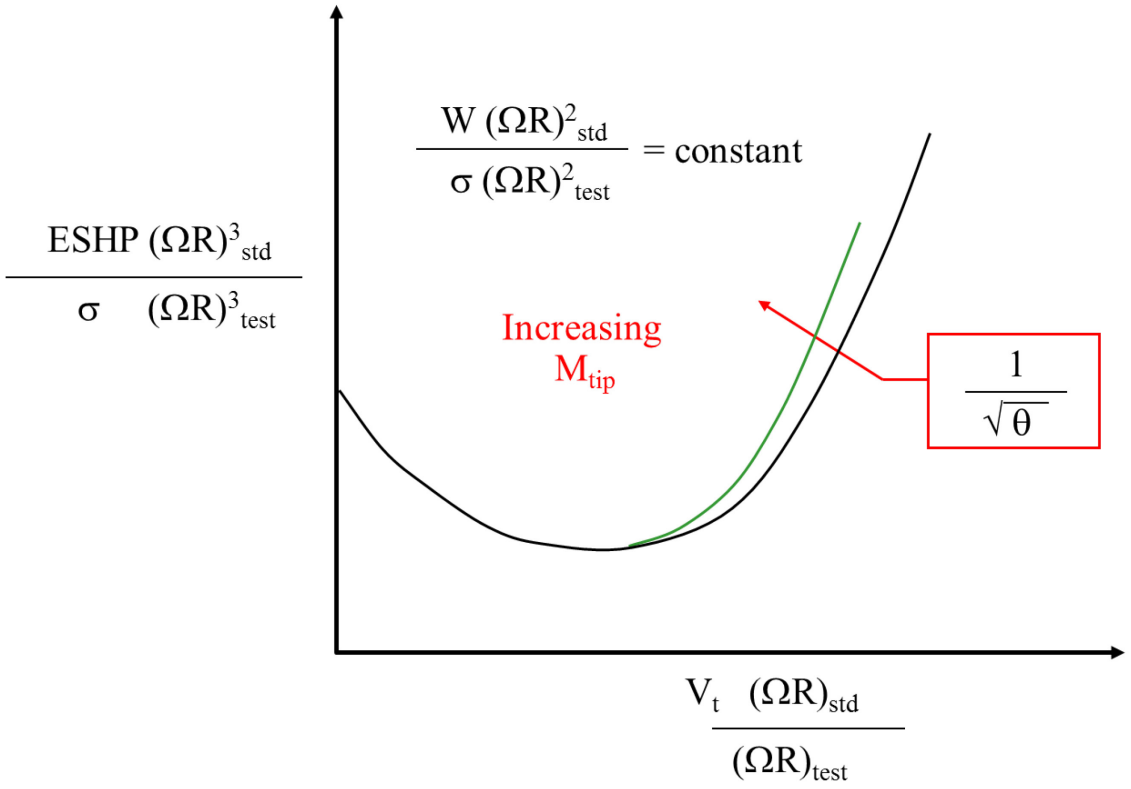

Figure 26: Constant W/σ Strategy for Determining Compressibility Effects.

8.0 SUMMARY

Established methods of performance testing and the performance models that are generated from those methods often fail to accurately represent the combined effects of weight and temperature extremes at high altitude. Alternate models exist with the capacity to more accurately represent the power required under these extreme conditions. A test team with the understanding of the physics and capacity behind both models can properly plan and execute a performance test program that provides the operator with products that ensure safe and effective operation in the extreme environment at high altitude. In doing so, the team must consider the following.

Test Location: Location will affect the ambient Temperature and Pressure available so early planning needs to ensure the range of conditions is obtainable. This will be based around the corrected data parameters that are required for validation of the operating performance for front line use or to meet specific test objectives. Site surveys to ensure appropriate facilities and security may be needed to form part of the test planning process.

Test Technique Selection: Selection of test method and corrected weight grouping to allow objective of the test to be met. Choosing W/δ or W/σ, means corrected mass and vertical performance techniques, such as free air or tethered hovering, will have a significant impact on the planning and instrumentation of the aircraft and support requirements. If investigating tip effects then the test team will need to modify the aircraft to enable rotor speed variation and control, with associated airworthiness approvals required for flight testing.

Aircraft Ballasting/Weight: Ballasting schemes to get the weight required to meet the corrected weight for test will need to be developed and should consider emergency operation such as weight reduction in emergencies (water ballast use), and crash cases for structural integrity on ballast installation. During testing the weight of the aircraft is critical to accurate data collection. Provisions should be made to weigh everything; including the aircraft, crew and anything on the aircraft that adds weight. Specific gravity of the fuel will also vary and needs to be accounted to ensure the team account for the changes in the weight of the fuel during testing. A good understanding of the operation of the aircraft's fuel indicating system is therefore also required.

External Configuration: The profile drag of the airframe is a key part of the performance of the rotorcraft and pictorial records of the external configuration of the test aircraft can provide an important record. In addition the engine intake and exhaust configuration will have a significant impact in the installed engine performance.

Instrumentation: Instrumentation to gather the data needed by the crew to achieve the data collection including engine parameters, fuel contents and flow rates, air data and aircraft flight parameters. Fuel flow instrumentation must meet requirements for accuracy of data and ensuring system is safe to operate. Strain gauging of rotor blades may be necessary to monitor structural stress during testing.

Engine Performance Standard: Engine calibration to ensure that the power output of the engine is accurately defined and may be needed pre and post-test to assist analysis of the data gathered and needs to be planned in the test program. Spare calibrated engines for failures or rejections should also be considered in test planning.

Test Sortie Planning: The test team should have planning charts to ensure that the required corrected data can be collected during the test sortie. Charts of the fuel gone/load and target corrected weight can be calculated to guide climbs between testing to ensure accurate data collection. Weather balloons may be used to identify non-standard ambient conditions may be used to adjust planning charts to the conditions of the day.

Data Quality: Time for rotor(s) and engine(s) to settle can mean long test points to reduce error and this time needs to be planned into the test profile to ensure accurate data can be obtained. The use of flight control system hold functions and their impact on performance data should be considered in test planning to ensure suitable performance data is collected.

Avionics/Systems Effects: The reduced mass flow at high altitudes may impact cooling of systems (avionic or air vehicle) and needs to be considered in test planning. Advice form equipment manufacturers may be needed.

Aircrew Safety and Survival Equipment: Training and equipment for extreme weather conditions and survival in the event of force landings in remote locations in extreme climates needs to be considered during early test planning. The use of parachutes and oxygen systems will also need to be considered depending upon the height above ground and pressure altitude the aircraft will be operated at.

Emergencies: Some high altitude testing may place the aircraft in abnormal and unusual flight conditions. Briefing for emergencies due to any test hazards, i.e. vortex ring or actions if an engine fails in an unusual rotor speed setting for example may need to be considered to understand the operating risks during test conduct and to ensure suitable mitigations and preparation are taken by the test team. Aircrew egress with personal and aircraft equipment should also be considered to ensure crews are able to evacuate the aircraft with abnormal and bulky equipment.

9.0 REFERENCES

[1] US Naval Test Pilot School Flight Test Manual 106, Rotary Wing Performance, Naval Air Warfare Center Patuxent River, MD, 1996.

[2] P&W Operating Instruction 200, The Aircraft Gas Turbine Engine and Its Operation, United Technologies, Pratt & Whitney, Part No. P&W 182408, August 1988.

[3] Basset, P., Chen, C., Prasad, J.V.R. and Kolb, S., Prediction of Vortex Ring State Boundary of a Helicopter in Descending Flight by Simulation, Journal of the American Helicopter Society, April 2008.

[4] Xin, H. and Gao, Z., A Prediction of the Vortex-Ring State Boundary Based on Model Tests, Transactions of Nanjing University of Aeronautics and Astronautics, Vol. 11, (2), December 1994, pp. 159-164.

[5] Xin, H. and Gao, Z., An Experimental Investigation of Model Rotors Operating in Vertical Descent, 19th European Rotorcraft Forum Proceedings, Cernobbio, Italy, September 14-16, 1993.

[6] Brand, A., Kisor, R., Blyth, R., Mason, D. and Host, C., V-22 High Rate of Descent (HROD) Test Procedures and Long Record Analysis, Presented at the American Helicopter Society 60th Annual Forum, Baltimore, MD, June 7-10, 2004.

[7] Brand, A., Kisor, R., Blyth, R. and MacDonald, T. V-22 Low-speed/High Rate of Descent (HROD) Test Results, Presented at the American Helicopter Society 60th Annual Forum, Baltimore, MD, June 7-10, 2004.

[8] Empire Test Pilot School Rotary Wing Flight Test Manual, QinetiQ/TES/ETPS/RWFTM, QinetiQ Ltd, 2006.

[9] Federal Aviation Administration Advisory Circular AC-29-2C, Certification of Transport Category Rotorcraft, Changes 1-6 Incorporated, September 2008.

Annex A – AGARD, RTO and STO Flight Test Instrumentation and Flight Test Techniques Series

1. Volumes in the AGARD, RTO and STO Flight Test Instrumentation Series, AGARDograph 160

Volume Number	Title	Publication Date
1.	Basic Principles of Flight Test Instrumentation Engineering (Issue 2) Issue 1: Edited by A. Pool and D. Bosman Issue 2: Edited by R. Borek and A. Pool	 1974 1994
2.	In-Flight Temperature Measurements by F. Trenkle and M. Reinhardt	1973
3.	The Measurements of Fuel Flow by J.T. France	1972
4.	The Measurements of Engine Rotation Speed by M. Vedrunes	1973
5.	Magnetic Recording of Flight Test Data by G.E. Bennett	1974
6.	Open and Closed Loop Accelerometers by I. McLaren	1974
7.	Strain Gauge Measurements on Aircraft by E. Kottkamp, H. Wilhelm and D. Kohl	1976
8.	Linear and Angular Position Measurement of Aircraft Components by J.C. van der Linden and H.A. Mensink	1977
9.	Aeroelastic Flight Test Techniques and Instrumentation by J.W.G. van Nunen and G. Piazzoli	1979
10.	Helicopter Flight Test Instrumentation by K.R. Ferrell	1980
11.	Pressure and Flow Measurement by W. Wuest	1980
12.	Aircraft Flight Test Data Processing – A Review of the State of the Art by L.J. Smith and N.O. Matthews	1980
13.	Practical Aspects of Instrumentation System Installation by R.W. Borek	1981
14.	The Analysis of Random Data by D.A. Williams	1981
15.	Gyroscopic Instruments and Their Application to Flight Testing by B. Stieler and H. Winter	1982
16.	Trajectory Measurements for Take-off and Landing Test and Other Short-Range Applications by P. de Benque D'Agut, H. Riebeek and A. Pool	1985

17.	Analogue Signal Conditioning for Flight Test Instrumentation by D.W. Veatch and R.K. Bogue	1986
18.	Microprocessor Applications in Airborne Flight Test Instrumentation by M.J. Prickett	1987
19.	Digital Signal Conditioning for Flight Test by G.A. Bever	1991
20.	Optical Air Flow Measurements in Flight by R.K. Bogue and H.W. Jentink	2003
21.	Differential Global Positioning System (DGPS) for Flight Testing by R. Sabatini and G.B. Palmerini	2008
22.	Application of Fiber Optic Instrumentation by L. Richards, A.R. Parker Jr., W.L. Ko, A. Piazza and P. Chan	2012

2. Volumes in the AGARD, RTO and STO Flight Test Techniques Series, AGARDograph 300

Volume Number	Title	Publication Date
AG237	Guide to In-Flight Thrust Measurement of Turbojets and Fan Engines by the MIDAP Study Group (UK)	1979

The remaining volumes are published as a sequence of Volume Numbers of AGARDograph 300.

1.	Calibration of Air-Data Systems and Flow Direction Sensors by J.A. Lawford and K.R. Nippress	1988
2.	Identification of Dynamic Systems by R.E. Maine and K.W. Iliff	1988
3.	Identification of Dynamic Systems – Applications to Aircraft Part 1: The Output Error Approach by R.E. Maine and K.W. Iliff Part 2: Nonlinear Analysis and Manoeuvre Design by J.A. Mulder, J.K. Sridhar and J.H. Breeman	 1986 1994
4.	Determination of Antenna Patterns and Radar Reflection Characteristics of Aircraft by H. Bothe and D. McDonald	1986
5.	Store Separation Flight Testing by R.J. Arnold and C.S. Epstein	1986
6.	Developmental Airdrop Testing Techniques and Devices by H.J. Hunter	1987
7.	Air-to-Air Radar Flight Testing by R.E. Scott	1992
8.	Flight Testing under Extreme Environmental Conditions by C.L. Henrickson	1988
9.	Aircraft Exterior Noise Measurement and Analysis Techniques by H. Heller	1991
10.	Weapon Delivery Analysis and Ballistic Flight Testing by R.J. Arnold and J.B. Knight	1992
11.	The Testing of Fixed Wing Tanker & Receiver Aircraft to Establish Their Air-to-Air Refuelling Capabilities by J. Bradley and K. Emerson	1992
12.	The Principles of Flight Test Assessment of Flight-Safety-Critical Systems in Helicopters by J.D.L. Gregory	1994
13.	Reliability and Maintainability Flight Test Techniques by J.M. Howell	1994
14.	Introduction to Flight Test Engineering Issue 1: Edited by F. Stoliker Issue 2: Edited by F. Stoliker and G. Bever	 1995 2005
15.	Introduction to Avionics Flight Test by J.M. Clifton	1996

16.	Introduction to Airborne Early Warning Radar Flight Test by J.M. Clifton and F.W. Lee	1999
17.	Electronic Warfare Test and Evaluation[‡] by H. Banks and R. McQuillan	2000
18.	Flight Testing of Radio Navigation Systems by H. Bothe and H.J. Hotop	2000
19.	Simulation in Support of Flight Testing by D. Hines	2000
20.	Logistics Test and Evaluation in Flight Testing by M. Bourcier	2001
21.	Flying Qualities Flight Testing of Digital Flight Control Systems by F. Webster and T.D. Smith	2001
22.	Helicopter/Ship Qualification Testing by D. Carico, R. Fang, R.S. Finch, W.P. Geyer Jr., Cdr. (Ret.) H.W. Krijns and K. Long	2002
23.	Flight Test Measurement Techniques for Laminar Flow by D. Fisher, K.H. Horstmann and H. Riedel	2003
24.	Precision Airdrop by M.R. Wuest and R.J. Benney	2005
25.	Flight Testing of Night Vision Systems in Rotorcraft by G. Craig, T. Macuda, S. Jennings, G. Ramphal and A. Stewart	2007[†]
26.	Airborne Laser Systems Testing and Analysis by R. Sabatini and M.A. Richardson	2010
27.	Unique Aspects of Flight Testing Unmanned Aircraft Systems by A.E. Pontzer, M.D. Lower and J.R. Miller	2010
28.	Electronic Warfare Test and Evaluation by M. Welch and M. Pywell	2012
29.	Aircraft/Stores Compatibility, Integration and Separation Testing by O. Nadar	2014
30.	High Altitude Rotary Wing Flight Testing – Considerations in Planning Rotary Wing Performance Testing for High Altitude Operations by J. O'Connor, J. McCue, J. Holder and B. Carrothers	2018

[‡] Superseded by Volume 28.

[†] Volume 25 has been published as RTO AGARDograph AG-SCI-089.

REPORT DOCUMENTATION PAGE

1. Recipient's Reference	2. Originator's References	3. Further Reference	4. Security Classification of Document
	STO-AG-300-V30 AC/323(SCI-255)TP/759	ISBN 978-92-837-2085-0	PUBLIC RELEASE

5. Originator

Science and Technology Organization
North Atlantic Treaty Organization
BP 25, F-92201 Neuilly-sur-Seine Cedex, France

6. Title

High Altitude Rotary Wing Flight Testing – Considerations in Planning Rotary Wing Performance Testing for High Altitude Operations

7. Presented at/Sponsored by

This AGARDograph has been sponsored by the Systems Concepts and Integration Panel.

8. Author(s)/Editor(s)	9. Date
Mr. John O'Connor, Mr. Jim McCue, LtCdr John Holder and Mr. Bryan Carrothers	February 2018
10. Author's/Editor's Address	**11. Pages**
Multiple	52

12. Distribution Statement

There are no restrictions on the distribution of this document. Information about the availability of this and other RTO unclassified publications is given on the back cover.

13. Keywords/Descriptors

Blade stall
Equivalent Retreating Tip Speed (ERiTS)
High altitude rotary wing flight test
Surge limit
Vortex ring state

14. Abstract

This AGARDograph presents an approach to modify the methods used to gather flight test data and generate helicopter performance charts. Present performance models do not address extremes of temperature at high altitudes found in present areas of operation. The combined effects of weight and temperature extremes at high altitude are often not captured by established methods of test. An explanation of the related aero-thermodynamic limits of the engine is developed and the implications in test planning are discussed. An explanation of the effects of weight, temperature, and pressure extremes on the limits of the rotor blade and resultant impacts on power required is also developed. Test methods for gathering data and finding the limits of power available and power required under the extreme conditions are presented along with the data reduction for analysis. The AGARDograph also develops and explains the use of energy management diagrams with the unique high altitude limits represented on the diagrams.

NORTH ATLANTIC TREATY ORGANIZATION

BP 25
F-92201 NEUILLY-SUR-SEINE CEDEX • FRANCE
Télécopie 0(1)55.61.22.99 • E-mail mailbox@cso.nato.int

SCIENCE AND TECHNOLOGY ORGANIZATION

DIFFUSION DES PUBLICATIONS

STO NON CLASSIFIEES

Les publications de l'AGARD, de la RTO et de la STO peuvent parfois être obtenues auprès des centres nationaux de distribution indiqués ci-dessous. Si vous souhaitez recevoir toutes les publications de la STO, ou simplement celles qui concernent certains Panels, vous pouvez demander d'être inclus soit à titre personnel, soit au nom de votre organisation, sur la liste d'envoi.

Les publications de la STO, de la RTO et de l'AGARD sont également en vente auprès des agences de vente indiquées ci-dessous.

Les demandes de documents STO, RTO ou AGARD doivent comporter la dénomination « STO », « RTO » ou « AGARD » selon le cas, suivi du numéro de série. Des informations analogues, telles que le titre est la date de publication sont souhaitables.

Si vous souhaitez recevoir une notification électronique de la disponibilité des rapports de la STO au fur et à mesure de leur publication, vous pouvez consulter notre site Web (http://www.sto.nato.int/) et vous abonner à ce service.

CENTRES DE DIFFUSION NATIONAUX

ALLEMAGNE
Streitkräfteamt / Abteilung III
Fachinformationszentrum der Bundeswehr (FIZBw)
Gorch-Fock-Straße 7, D-53229 Bonn

BELGIQUE
Royal High Institute for Defence – KHID/IRSD/RHID
Management of Scientific & Technological Research
for Defence, National STO Coordinator
Royal Military Academy – Campus Renaissance
Renaissancelaan 30, 1000 Bruxelles

BULGARIE
Ministry of Defence
Defence Institute "Prof. Tsvetan Lazarov"
"Tsvetan Lazarov" bul no.2
1592 Sofia

CANADA
DGSIST 2
Recherche et développement pour la défense Canada
60 Moodie Drive (7N-1-F20)
Ottawa, Ontario K1A 0K2

DANEMARK
Danish Acquisition and Logistics Organization
(DALO)
Lautrupbjerg 1-5
2750 Ballerup

ESPAGNE
Área de Cooperación Internacional en I+D
SDGPLATIN (DGAM)
C/ Arturo Soria 289
28033 Madrid

ESTONIE
Estonian National Defence College
Centre for Applied Research
Riia str 12
Tartu 51013

ETATS-UNIS
Defense Technical Information Center
8725 John J. Kingman Road
Fort Belvoir, VA 22060-6218

FRANCE
O.N.E.R.A. (ISP)
29, Avenue de la Division Leclerc
BP 72
92322 Châtillon Cedex

GRECE (Correspondant)
Defence Industry & Research General
Directorate, Research Directorate
Fakinos Base Camp, S.T.G. 1020
Holargos, Athens

HONGRIE
Hungarian Ministry of Defence
Development and Logistics Agency
P.O.B. 25
H-1885 Budapest

ITALIE
Centro Gestione Conoscenza
Secretariat General of Defence
National Armaments Directorate
Via XX Settembre 123/A
00187 Roma

LUXEMBOURG
Voir Belgique

NORVEGE
Norwegian Defence Research
Establishment
Attn: Biblioteket
P.O. Box 25
NO-2007 Kjeller

PAYS-BAS
Royal Netherlands Military
Academy Library
P.O. Box 90.002
4800 PA Breda

POLOGNE
Centralna Biblioteka Wojskowa
ul. Ostrobramska 109
04-041 Warszawa

PORTUGAL
Estado Maior da Força Aérea
SDFA – Centro de Documentação
Alfragide
P-2720 Amadora

REPUBLIQUE TCHEQUE
Vojenský technický ústav s.p.
CZ Distribution Information Centre
Mladoboleslavská 944
PO Box 18
197 06 Praha 9

ROUMANIE
Romanian National Distribution
Centre
Armaments Department
9-11, Drumul Taberei Street
Sector 6
061353 Bucharest

ROYAUME-UNI
Dstl Records Centre
Rm G02, ISAT F, Building 5
Dstl Porton Down
Salisbury SP4 0JQ

SLOVAQUIE
Akadémia ozbrojených síl gen.
M.R. Štefánika, Distribučné a
informačné stredisko STO
Demänová 393
031 06 Liptovský Mikuláš 6

SLOVENIE
Ministry of Defence
Central Registry for EU & NATO
Vojkova 55
1000 Ljubljana

TURQUIE
Milli Savunma Bakanlığı (MSB)
ARGE ve Teknoloji Dairesi
Başkanlığı
06650 Bakanliklar – Ankara

AGENCES DE VENTE

The British Library Document Supply Centre
Boston Spa, Wetherby
West Yorkshire LS23 7BQ
ROYAUME-UNI

Canada Institute for Scientific and Technical Information (CISTI)
National Research Council Acquisitions
Montreal Road, Building M-55
Ottawa, Ontario K1A 0S2
CANADA

Les demandes de documents STO, RTO ou AGARD doivent comporter la dénomination « STO », « RTO » ou « AGARD » selon le cas, suivie du numéro de série (par exemple AGARD-AG-315). Des informations analogues, telles que le titre et la date de publication sont souhaitables. Des références bibliographiques complètes ainsi que des résumés des publications STO, RTO et AGARD figurent dans le « NTIS Publications Database » (http://www.ntis.gov).

NORTH ATLANTIC TREATY ORGANIZATION

BP 25
F-92201 NEUILLY-SUR-SEINE CEDEX • FRANCE
Télécopie 0(1)55.61.22.99 • E-mail mailbox@cso.nato.int

SCIENCE AND TECHNOLOGY ORGANIZATION

DISTRIBUTION OF UNCLASSIFIED STO PUBLICATIONS

AGARD, RTO & STO publications are sometimes available from the National Distribution Centres listed below. If you wish to receive all STO reports, or just those relating to one or more specific STO Panels, they may be willing to include you (or your Organisation) in their distribution.

STO, RTO and AGARD reports may also be purchased from the Sales Agencies listed below.

Requests for STO, RTO or AGARD documents should include the word 'STO', 'RTO' or 'AGARD', as appropriate, followed by the serial number. Collateral information such as title and publication date is desirable.

If you wish to receive electronic notification of STO reports as they are published, please visit our website (http://www.sto.nato.int/) from where you can register for this service.

NATIONAL DISTRIBUTION CENTRES

BELGIUM
Royal High Institute for Defence – KHID/IRSD/RHID
Management of Scientific & Technological Research for Defence, National STO Coordinator
Royal Military Academy – Campus Renaissance
Renaissancelaan 30
1000 Brussels

BULGARIA
Ministry of Defence
Defence Institute "Prof. Tsvetan Lazarov"
"Tsvetan Lazarov" bul no.2
1592 Sofia

CANADA
DSTKIM 2
Defence Research and Development Canada
60 Moodie Drive (7N-1-F20)
Ottawa, Ontario K1A 0K2

CZECH REPUBLIC
Vojenský technický ústav s.p.
CZ Distribution Information Centre
Mladoboleslavská 944
PO Box 18
197 06 Praha 9

DENMARK
Danish Acquisition and Logistics Organization (DALO)
Lautrupbjerg 1-5
2750 Ballerup

ESTONIA
Estonian National Defence College
Centre for Applied Research
Riia str 12
Tartu 51013

FRANCE
O.N.E.R.A. (ISP)
29, Avenue de la Division Leclerc – BP 72
92322 Châtillon Cedex

GERMANY
Streitkräfteamt / Abteilung III
Fachinformationszentrum der Bundeswehr (FIZBw)
Gorch-Fock-Straße 7
D-53229 Bonn

GREECE (Point of Contact)
Defence Industry & Research General Directorate, Research Directorate
Fakinos Base Camp, S.T.G. 1020
Holargos, Athens

HUNGARY
Hungarian Ministry of Defence
Development and Logistics Agency
P.O.B. 25
H-1885 Budapest

ITALY
Centro Gestione Conoscenza
Secretariat General of Defence
National Armaments Directorate
Via XX Settembre 123/A
00187 Roma

LUXEMBOURG
See Belgium

NETHERLANDS
Royal Netherlands Military Academy Library
P.O. Box 90.002
4800 PA Breda

NORWAY
Norwegian Defence Research Establishment, Attn: Biblioteket
P.O. Box 25
NO-2007 Kjeller

POLAND
Centralna Biblioteka Wojskowa
ul. Ostrobramska 109
04-041 Warszawa

PORTUGAL
Estado Maior da Força Aérea
SDFA – Centro de Documentação
Alfragide
P-2720 Amadora

ROMANIA
Romanian National Distribution Centre
Armaments Department
9-11, Drumul Taberei Street
Sector 6
061353 Bucharest

SLOVAKIA
Akadémia ozbrojených síl gen M.R. Štefánika, Distribučné a informačné stredisko STO
Demänová 393
031 06 Liptovský Mikuláš 6

SLOVENIA
Ministry of Defence
Central Registry for EU & NATO
Vojkova 55
1000 Ljubljana

SPAIN
Área de Cooperación Internacional en I+D
SDGPLATIN (DGAM)
C/ Arturo Soria 289
28033 Madrid

TURKEY
Milli Savunma Bakanlığı (MSB)
ARGE ve Teknoloji Dairesi Başkanlığı
06650 Bakanliklar – Ankara

UNITED KINGDOM
Dstl Records Centre
Rm G02, ISAT F, Building 5
Dstl Porton Down, Salisbury SP4 0JQ

UNITED STATES
Defense Technical Information Center
8725 John J. Kingman Road
Fort Belvoir, VA 22060-6218

SALES AGENCIES

The British Library Document Supply Centre
Boston Spa, Wetherby
West Yorkshire LS23 7BQ
UNITED KINGDOM

Canada Institute for Scientific and Technical Information (CISTI)
National Research Council Acquisitions
Montreal Road, Building M-55
Ottawa, Ontario K1A 0S2
CANADA

Requests for STO, RTO or AGARD documents should include the word 'STO', 'RTO' or 'AGARD', as appropriate, followed by the serial number (for example AGARD-AG-315). Collateral information such as title and publication date is desirable. Full bibliographical references and abstracts of STO, RTO and AGARD publications are given in "NTIS Publications Database" (http://www.ntis.gov).

ISBN 978-92-837-2085-0